Earth and Planetary Science Letters 564 (2021) 116893

Contents lists available at ScienceDirect

Earth and Planetary Science Letters

www.elsevier.com/locate/epsl

Evidence for crustal removal, tectonic erosion and flare-ups from the Japanese evolving forearc sediment provenance

Daniel Pastor-Galán [a,b,c,*], Christopher J. Spencer [d,e], Tan Furukawa [c], Tatsuki Tsujimori [b,c]

[a] Frontier Research Institute for Interdisciplinary Science, Tohoku University, Japan
[b] Center for North East Asian Studies, Tohoku University, 980-8576, 41 Kawauchi, Aoba-ku, Sendai, Miyagi, Japan
[c] Department of Earth Science, Graduate School of Science, Tohoku University, Japan
[d] School of Earth and Planetary Sciences, The Institute for Geoscience Research (TIGeR), Curtin University, Perth, Australia
[e] Department of Geological Sciences and Geological Engineering, Queen's University, Kingston, Canada

ARTICLE INFO

Article history:
Received 15 October 2020
Received in revised form 11 March 2021
Accepted 15 March 2021
Available online 6 April 2021
Editor: R. Hickey-Vargas

Keywords:
detrital zircon
geochronology
Lu-Hf
crustal growth
tectonic erosion

ABSTRACT

Forearc basins preserve the geologic record relating strictly to arc magmatism. The provenance of forearc sediment can be used to differentiate periods of crustal growth, accretion, and destruction, enhanced magmatism, advancing and retreating subduction slabs, delamination, etc. These tectonic systems predict differing degrees of sedimentary reworking of the older forearc units. Additionally, Hf isotopes of zircon can be used to evaluate the degree of continental reworking that occurs in the arc system. In this paper, we evaluate the changes in a long-lived subduction system using detrital zircon U-Pb and Hf-isotope data from forearc units in northern Honshu, Japan that span in age from the Silurian Period to the present from the forearc provenance of the Japanese subduction system. Our data demonstrate a series of dominant age peaks (430 ± 20, 360 ± 10, 270 ± 20, 184 ± 12, 112 ± 22, and 7 ± 7 Ma) and a progressive loss of the older zircon populations. Zircon Hf-isotope data reveal three discrete shifts that correspond to differing degrees of isotopic enrichment and correlate with changes in the dominant zircon age peaks. Additionally, each temporal isotopic shift is associated with isolation of the older sedimentary packages wherein no detrital zircon from the previous stages are observed in subsequent stages. We propose these shifts provide evidence for rapid shifts in arc tectonics including magmatic flare-ups, producing the dominant peaks; protracted tectonic erosion progressively removing older sources of zircon reveals a late Carboniferous event triggering the complete removal of the Precambrian crust; and the Cretaceous melting of the entire Permian arc crust, likely related with the subduction of the mid-oceanic ridge separating the Izanagi and Pacific plates.

1. Introduction

The history of the Earth, since the Archean, is carved in the continents' crustal records: the earliest rocks differentiated from the mantle; the origin, evolution of life; the evolution of the magnetic field, or the development of superplumes from the core-mantle boundary. Unfortunately, this information is disrupted and fragmented, the crust not only grows but recycles back into the mantle by a variety of processes. The continental crust grows by magmatism in arcs (e.g. Spencer et al., 2017), whereas it gets destroyed primarily in subduction zones through subduction of sediments, tectonic erosion (a.k.a. subduction erosion, von Huene and Lallemand, 1990), and lithospheric delamination *sensu lato* (e.g. Magni and Király, 2020). Tectonic erosion is the removal of upper-plate material from the forearc at convergent margins, originally proposed in the Japan and Peru Trenches by von Huene and Lallemand (1990). The global budget of continental crust has not been always neutral and there have been episodes of net growth and shrinkage (e.g. Spencer et al., 2019). Interestingly, during the episodes of net growth parts of the crust may have been vigorously destroyed and vice versa. Documenting the origin and fate of the continental crust is a key goal of the Earth sciences to understanding Earth's chemical evolution and the main tectonic processes operating through time. Sialic crustal growth and destruction are crucial to develop accurate plate restorations and paleogeography, which in turn are the foundation of Earth history, paleoclimatic studies, and tectonic research. Without accurate constraints of when and where a piece of crust existed such reconstructions are useless for their primary purpose.

The Panthalassa–Pacific ocean system has been subducting below today's East Asia–Oceania for at least 500 m.yrs (e.g.

* Corresponding author.
E-mail address: dpastorgalan@gmail.com (D. Pastor-Galán).

https://doi.org/10.1016/j.epsl.2021.116893
0012-821X/

Maruyama and Seno, 1986; Isozaki et al., 2010). The consumption of this superocean formed two of the largest accretionary orogens of the Phanerozoic where the continental crust grew significantly from ~1000 to 250 Ma: the Central Asian Orogenic Belt (Jahn, 2004) and ~800 to 250 Ma in the Terra Australis Orogen (Cawood, 2005). In contrast, the Japan arc is a narrow strip with a cyclic record fragmented accretionary complexes and blueschist (*s.l.*) exhumation during ~500 m. yr. of subduction preserved over a Cretaceous granitic crust. Although tectonic erosion has played an important role in the poor preservation of the Japanese basement (e.g. Isozaki et al., 2010), this process has been common in growing orogens (e.g. Stern, 2011). The reasons why the Japan arc behaved so differently to its counterparts in the Panthalassa–Pacific subduction zone are poorly known due to the discontinuity, large gaps, and scarcity of its crustal record.

Forearc basins preserve the geologic record relating strictly to arc magmatism where the bulk of the continental crust is created and destroyed. Although sediment from the volcanic arc is transported both to the backarc and forearc regions, the forearc is less likely to receive detritus from the hinterland as the magmatic arc often forms a continental divide. In this study, we investigate the crustal evolution of the northern Honshu arc (NE Japan) from the Silurian to the present day through the provenance of detrital zircon and their Hf-isotope signature in the South Kitakami forearc basin, which contains a close to continuous sedimentary record (cf. Ehiro et al., 2016). Our new results, together with a reappraisal of former studies, show a fierce history of periodic flare-ups, tectonic erosion, complete removal of the Precambrian crust in the late Carboniferous, and total melting of the Permian crust in the Cretaceous.

2. Geological background

The Japanese archipelago is a 3000 km long bow-shaped chain of islands along the eastern margin of Asia preserving at least 500-million-year history of subduction processes (e.g. Maruyama et al., 1997; Isozaki et al., 2010). At present, it is located at the junctions of four distinct plates Eurasian, Pacific, North American, and Philippine Sea plates (Fig. 1). The Pacific plate is subducting at a rate of ~8 cm/yr beneath NE Japan, whereas the Philippine Sea plate is subducting from SE to NW with ~3–5 cm/yr under SW Japan along the Nankai trough (trench) and Ryukyu trench off SW Japan.

2.1. Geological history of Japan

The origins of the present-day archipelago are tied to the breakup of the supercontinent Rodinia (e.g. Maruyama et al., 1997; Pastor-Galán et al., 2019), in particular to both North and South China cratons that rifted apart from Rodinia while Panthalassa ocean (paleo-Pacific) opened (e.g. Isozaki et al., 2010). After an uncertain period of Precambrian evolution, an ocean (perhaps the Panthalassa) commenced subduction below what today is the Japan arc. The oldest subduction-related rocks in both NW and SW Japan arcs are late Cambrian arc-type granitoids and serpentinized mantle wedge peridotites with jadeitites (e.g. Isozaki et al., 2015; Tsujimori, 2017). Despite their paucity and dismembered nature, they indicate the subduction history of Japan commenced at least ~500 Ma. It has been postulated that the proto-Japan arc formed part of eastern Cathaysia passive margin (Fig. 1) from late Proterozoic to early Paleozoic until subduction initiated or flipped in polarity during late Cambrian. This hypothesis is grounded on the fact that the majority of the Paleozoic stratigraphy of Japan suggest a connection with Cathaysia (e.g. Isozaki et al., 2010; Isozaki, 2019; Wakita et al., 2021). Some authors suggested, however, that parts of Japan (e.g. Hitachi, Akiyoshi, Ultra-Tamba) show robust coincidences with North China Craton and at least these areas may have originated there (Tagiri et al., 2011; Wakita et al., 2021). Finally, some researchers think that the Japanese crust could be a fragment from NE Gondwana that migrated northwards during the opening of the Neotethys (Permian) as an oceanic island arc to finally collide with both North and South China (Otoh et al., 1990; Okawa et al., 2013).

From late Ordovician, the same subduction regime apparently continued until the present time. Firstly as a continental arc to finally develop a small-scale back-arc basin with a minimal formation of true oceanic crust (Japan Sea) during the Miocene (e.g. Maruyama et al., 1997). The only continent-continent collision record in Japan is found in the Hida Belt, an allochthonous unit was thrusted over pre-Jurassic units during the Triassic collisional orogeny that sutured North and South China cratons (e.g. Isozaki, 1997; Ernst et al., 2007; Fig. 1). The absence of evidence for other collisional events supports a Panthalassa-Pacific facing arc from the Ordovician attached to the South China margin (e.g. Isozaki et al., 2014) rather than a Gondwana derived Tethyan facing arc colliding against China (Okawa et al., 2013).

The geotectonic units of present-day Japan archipelago are divided into SW and NE Japan by the Tanakura Tectonic line (Fig. 1). SW Japan is characterized by a series of orogen-parallel accretionary complexes; the Median Tectonic Line further separates the inner and outer zones. The overall structure is a pile of north-rooting subhorizontal nappes, whose older sheets usually occupy the upper structural positions. Voluminous calc-alkaline granitic batholiths with low-pressure/high-temperature (LP-HT) metamorphic rocks intruded the nappe structure in Cretaceous times, gently folding them to form synform-antiform structures. This magmatic event has been interpreted as a flare-up caused by the subduction of a mid-ocean ridge (Maruyama and Seno, 1986). In contrast, the nappe distribution in NE Japan is geometrically more complex due to significant structural complications (Fig. 2) together with a thick cover of Cenozoic volcanic rocks and sediments. Exposures of pre-Jurassic geotectonic units and Cretaceous batholiths in NE Japan are limited and occur mainly in the Kitakami and Abukuma Mountains. Although the subhorizontal nappe-pile structure is completely disrupted by N-S tending high angle faults, all lithological components in NE Japan are comparable to those of SW Japan (e.g., Isozaki et al., 2010).

In the ~500 Myr orogenic history (Fig. 1), the processes of accretion have been, apparently, episodic at Carboniferous; Late Permian, which included the collision of an oceanic arc; Jurassic; and Late Cretaceous to the present (e.g. Isozaki et al., 2010). Several fragments of serpentinized mantle wedge peridotites/serpentinites and intra-oceanic crust–mantle successions have been described: ~540 Ma (Oeyama and Miyamori–Hayachine), ~280 Ma (Yakuno), Late Jurassic (Mikabu and Horokanai), Late Cretaceous (Poroshiri) and Cretaceous-Eocene crystallization ages (Mineoka) (e.g., Ishiwatari and Tsujimori, 2003). In addition to these rocks, three high-pressure/low-temperature (HP-LT) metamorphic belts crop-out with ages of 360–300 Ma (Renge), 240–200 Ma (Suo), and 120–60 Ma (Sanbagawa and Kamuikotan) (Tsujimori and Itaya, 1999). Notably, the Renge and the equivalents HP-LT rocks occur in the serpentinite mélange associated with the Oeyama and Miyamori–Hayachine units, and 120–60 Ma HP-LT rocks in the inner zone of SW Japan are well paired with granitic batholiths and LP-HT metamorphic rocks in the inner zone (Miyashiro, 1961; Fig. 1).

A very particular feature of the present-day arc crust in Japan is that it is mostly Cretaceous or younger. Crustal-scale seismic cross-section of SW Japan reveal pre-Cretaceous rocks that occur as roof pendant at shallow depths (e.g. Ito et al., 2009). Despite the 400 m.yrs of pre-Cretaceous subduction history, pre-Cretaceous

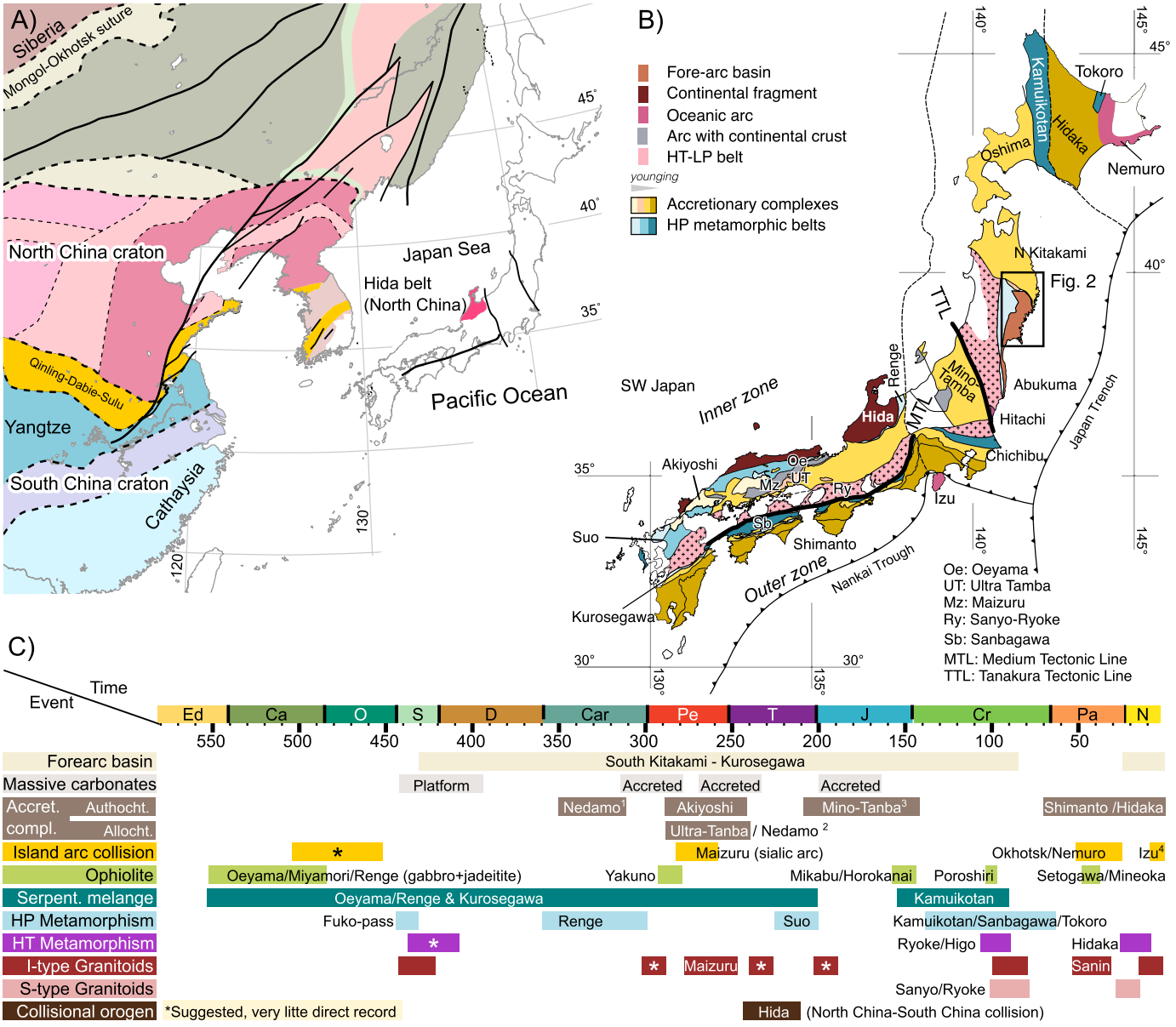

Fig. 1. A) Location of the main continental blocks and cratons of East Asia (modified after Harada et al., 2021). [1]Early Carboniferous Tsunatori Unit (Uchino, 2021); [2]Permian Takinosawa Unit (Uchino, 2021); [3]Including N Kitakami, Oshima and S Chichibu; [4]Including Kuril and Palau collisions. B) Simplified geological map of Japan based on the Seamless digital geological map of Japan 1: 200,000 (Geological Survey of Japan, 2021). C) Simplified chronology of the main tectonic events recorded in the Japanese active margin. (For interpretation of the colors in the figure(s), the reader is referred to the web version of this article.)

plutonic rocks are very scarce. Exposure of ~500–400 Ma granites are limited as fragments in the Kurosegawa Belt that is a klippe-like narrow composite unit in the outer zone of SW Japan and fault-bounded small blocks of the Kitakami Mountains of NE Japan (e.g. Isozaki et al., 2015; Shimojo et al., 2010). The best exposure of these granitic bodies is the Hikami Granite (Fig. 2 and SF-1) formed ~450–440 Ma (e.g. Shimojo et al., 2010; Isozaki et al., 2015). The ~300–270 Ma granites are extremely rare, and ~250–200 Ma granitoids only occur within the Hida Belt in central Japan. Several authors, primarily based on detrital zircon U-Pb ages studies, speculated that the pre-existing older arc crusts had been significantly removed, probably subducted into the mantle, by multiple episodes of tectonic erosion (e.g. Suzuki et al., 2010; Aoki et al., 2012). This secondary disappearance of older crust contributed to the shortage of information for paleogeographic reconstruction of Paleozoic and older Japan.

2.2. Geology of the South Kitakami Mountains

The South Kitakami Mountains (SKM hereafter) lie in Tohoku (NE Honshu, Fig. 2) and contain the only relatively thick Paleozoic and Mesozoic continental margin forearc basin in Japan. In the SKM also crop out some of the scarce Cambrian-Silurian arc granitoids (Isozaki et al., 2015); a weakly metamorphosed accretionary complex (the Motai metamorphic rocks, locally blueschist-facies), which has been compared to the Renge HP-LT metamorphic rocks of the SW Japan (Tsujimori and Itaya, 1999); and a supra-subduction zone ophiolite (Hayachine–Miyamori Complex; Ozawa et al., 2015). The South Kitakami forearc basin (SKFB hereafter) represent an independent tectonostratigraphic unit that contains a nearly continuous forearc sequence from Silurian to Early Cretaceous that lies over the Hikami granite and in tectonic contact with the accretionary and metamorphic units.

The SKFB comprises unmetamorphosed shallow-marine Silurian to Early Cretaceous strata (Fig. 1). The succession (Ehiro et al., 2016 and references therein) starts with a basal arkose overlain by Silurian limestone and tuff to Devonian tuff and interlayered mud- and sandstone. Those are unconformably overlain by the Early Carboniferous interlayered mud- and sandstone with some tuffaceous rocks followed by massive late Carboniferous limestones. Over a minor unconformity, Permian shallow marine clastic strata with volcaniclastics, limestones, and conglomeratic intercalations occur. The Mesozoic strata (Triassic to lowest Cretaceous) are located in the southern part of the SKM and were deposited in a shallow marine or alluvial environment and are mainly composed of clastic rocks in association with rare limestone and tuff. The Mesozoic stratigraphy starts over a disconformity with the Paleozoic strata and contains several minor unconformities (Fig. 2). This succession ends with a thick volcanic sequence at the Lower Cretaceous (Ehiro et al., 2016) and was intensively intruded during the Aptian-Albian (Fig. 1; e.g. Tsuchiya et al., 2014; Osozawa et al., 2019). The Aptian-Albian Cretaceous granitoids of the SKM show frequently adakitic or shoshonitic composition and ages ranging from 127–113 Ma (e.g. Osozawa et al., 2019; SF-1). These plutons are slightly older than the equivalent Cretaceous granitoids exposed in SW Japan.

Previous detrital zircon studies in the SKM (Shimojo et al., 2010; Okawa et al., 2013; Isozaki et al., 2014) tried to unravel the enigmatic pre-Mesozoic paleogeography of Japan through sediment provenance with contrasting results. The studies found a paucity of Precambrian zircon, which corroborates the forearc setting, where little sediment support from the continent is expected, but in turn, prevents paleogeographic correlations. Okawa et al. (2013) suggested the affinity of the SKM with Gondwana. In contrast, Isozaki et al. (2014, 2015) emphasized similarities of SKM, SW Japan, and E Russia with the South China block, supporting the hypothesis of a 'Greater South China Craton'.

3. Sampling, methods, and results

Fourteen fore-arc sedimentary clastic samples with ages from Silurian to present-day and one igneous sample (Hikami pluton, late Ordovician–early Silurian) were collected from the SKM of NE Honshu (Samples coded Kita; Fig. 2, Supplementary File SF-1). Biostratigraphic constraints demonstrate the age of sedimentary units spanning from the Silurian Period to the present (Fig. 2 and SF-1 for in detail rock formation). Zircon extraction followed traditional mineral separation techniques (crushing, milling, sieving, Wilfley table, Franz magnetic separation, and heavy liquid separation). Zircon were mounted in epoxy, imaged with cathodoluminescence, and analyzed for U-Pb and Hf-isotopes during two sessions via laser ablation inductively coupled plasma mass spectrometry (LA-ICP-MS) in the John de Laeter Centre (JdLC) at Curtin University with a Resonetics RESOlution M-50A-LR, incorporating a Compex 102 excimer laser. Following a 15–20 s period of background analysis, samples were spot ablated for 30 s at a 7 Hz repetition rate using a 33 µm beam and laser energy of 1.7 J/cm^2 at the sample surface. The sample cell was flushed by ultrahigh purity He (0.68 L min^{-1}) and N2 (2.8 mL min^{-1}). Isotopic intensities were measured using an Agilent 7700s quadrupole ICP-MS and a Nu Instruments Plasma II MC-ICP-MS, with high purity Ar as the plasma gas (flow rate 0.98 L min^{-1}). On the quadrupole, most elements were monitored for 0.01 s each with the exception of ^{88}Sr (0.02 s), ^{139}La (0.04 s), ^{141}Pr (0.04 s), ^{204}Pb, ^{206}Pb, ^{207}Pb, ^{208}Pb (all Pb 0.03 s), ^{232}Th (0.0125 s), and ^{238}U (0.0125 s). Approximately half of the split was sent to a Nu Plasma II MC-ICP-MS for Lu–Hf isotopic measurement. Masses for ^{172}Yb, ^{173}Yb, ^{175}Lu, ^{176}Hf + Yb + Lu, ^{177}Hf, ^{178}Hf, ^{179}Hf, and ^{180}Hf were measured simultaneously. Concordant zircon ages were defined as those for which the calculated ages from two U–Pb systems lie within uncertainty of one another (Spencer et al., 2016). Propagated uncertainties larger than 10% were considered unreasonable and these data were excluded. εHf(t) values were calculated for all data using the ^{176}Lu decay constant = $1.865 \times 10 - 11$ yr^{-1} (Scherer et al., 2001). Chondritic values are after Bouvier et al. (2008); ^{176}Hf/^{177}Hf CHUR = 0.282785, ^{176}Lu/^{177}Hf CHUR = 0.0336. Depleted mantle values ^{176}Hf/^{177}Hf = 0.28325, ^{176}Lu/^{177}Hf = 0.0384 after Griffin et al. (2000). For zircon grains with ages <1,500 Ma, the ^{206}Pb/^{238}U age was used, while for zircon >1,500 Ma, the ^{207}Pb/^{206}Pb age was used Spencer et al. (2016). Further technical details regarding standards and reduction of results in included in the supplemental File SF1.

We have complemented our dataset with 18 Paleozoic and Mesozoic U–Pb detrital zircon samples from Okawa et al. (2013) (16 Samples newly coded OK) and Isozaki et al. (2014) (2 samples newly coded IS; Fig. 2; full site description in SF-1). In addition, we also show the zircon U–Pb from 8 plutons that intruded the fore-arc basin of SK (Plutons newly coded OSO after Osozawa et al., 2019). Five out of these eight plutonic units also include Hf-isotope analyses in zircon: one from Hikami granite and four from Aptian-Albian plutons (Tono, Hondera, Kesengawa, and Hitokabe; Fig. 2; SF-1). We used the software package BAD-ZUPA (SF1-3) to quantitatively study the dominant zircon populations in the detrital zircon spectra, in addition to kernel density estimations and multi-dimensional scaling (Vermeesch, 2018). BAD-ZUPA is capable of automatically identifying the statistically significant peaks and valleys (at a 95% confidence), their most probable age, and the uncertainty of it.

Our sample from Hikami Granite (Kita13) displays no inherited zircon and a weighted average age of 435 ± 2.3 Ma (SF1). This age is compatible with previously published ages from U-Pb in zircon (OSO-08 in SF1, 442.4 ± 9.8 Ma, and 449.2 ± 4.5 Ma, Osozawa et al., 2019) and other methods (Ehiro et al., 2016 and references therein). Cretaceous granitoids samples from Osozawa et al. (2019: OSO-01 to OSO-07) show ages between 120 and 110 Ma (see SF1).

In general terms, detrital zircon age spectra of samples from the Kitakami forearc present unimodal or bimodal age distributions whose main peak is increasingly young in tandem with the stratigraphy (Fig. 3). With the single exception of the Orikabetoge formation (Kita17, IS1) the maximum depositional ages, defined by the youngest concordant analysis, are in line with the biostratigraphic constraints (Fig. 3). Silurian and Devonian samples (Kita17, 12, 07; OK1-3 and IS1) have a unimodal distribution with a late Silurian to early Devonian maxima, similar to the ages from Hikami granite. Carboniferous samples Kita06 and OK4 are bimodal with the former late Silurian peak and a major Carboniferous one (~355 Ma) whereas IS2 show a wide unimodal distribution with a peak in 356 but including the Silurian-Devonian maxima in the distribution. All Permo-Triassic samples (Kita16, 11, 02, 05, and OK5-10) are unimodal with a Permian (290-260 Ma) peak except for OK10 (Late Triassic), which shows a minor Triassic peak. Jurassic and Cretaceous samples are unimodal (OK11, Kita04, 15), bimodal (OK12, 13, Kita10, 01), or multimodal (OK14 and 16). The Permian peak is represented in all the samples and an early Jurassic one (~190–180 Ma) is common to all but OK11 and Kita04. The youngest Cretaceous sample (OK16) shows a Cretaceous peak (~130 Ma). The Cenozoic samples present a prominent Cretaceous peak (~105 Ma) with ages similar to the SKM Cretaceous granitoids and a smaller sub-recent peak (with zircon ages from Miocene to Quaternary). Precambrian zircon are statistically not relevant, 12 samples contained 0 Precambrian zircon, and the others just a few, which never cluster. These Precambrian zircon occur mostly in pre-Permian, Jurassic, and Cretaceous samples. Age spectra and a composite spectrum with all samples (Figs. 3 and 4) show that younger populations contain very little to no zircon from the oldest representative peak. This is especially noticeable in

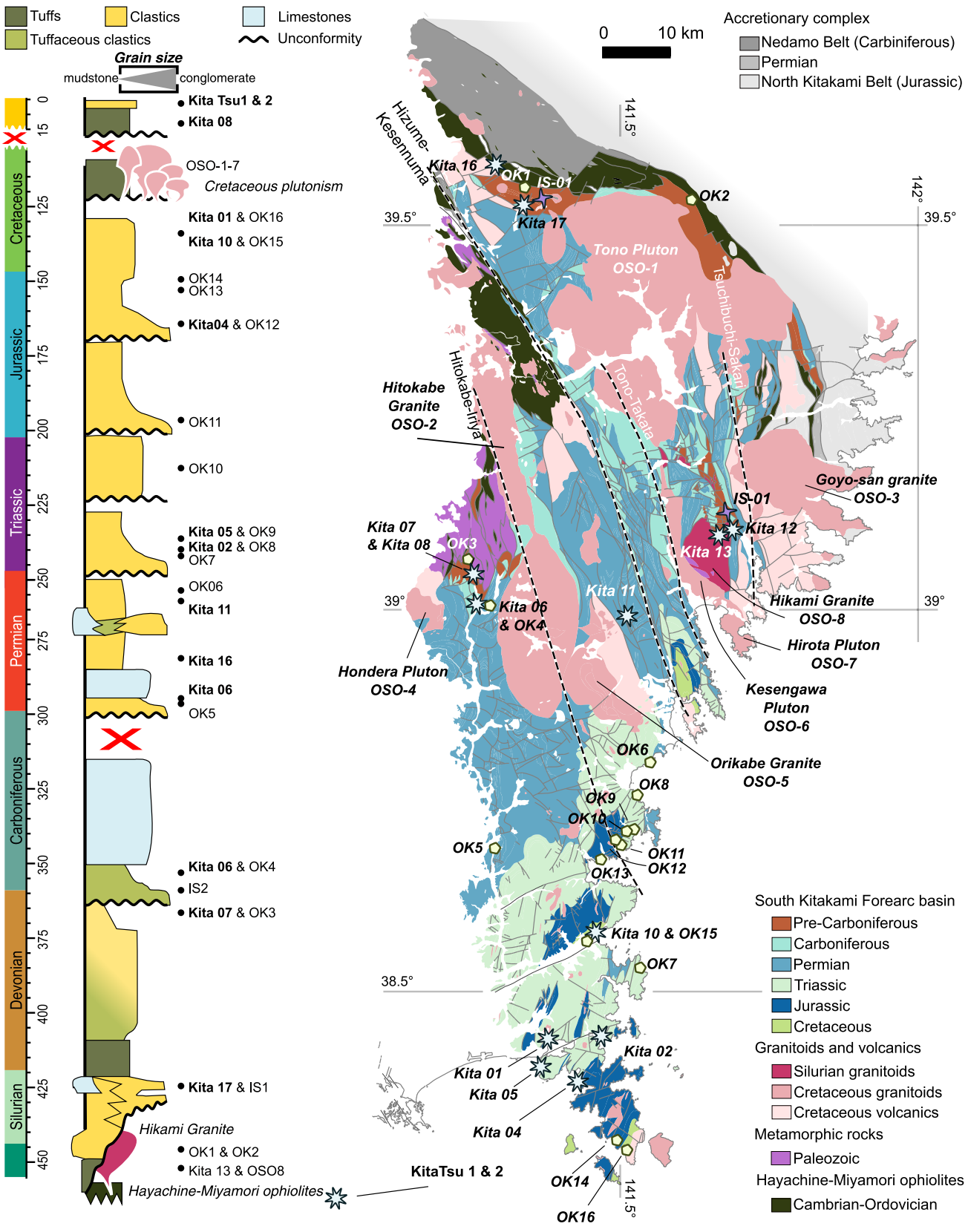

Fig. 2. South Kitakami synthetic geological map and stratigraphy showing the sampling locations based on the Seamless digital geological map of Japan 1: 200,000 (Geological Survey of Japan, 2021). Samples coded Kita are newly analyzed, OK after Okawa et al. (2013), IS after Isozaki et al. (2014) and samples coded OSO after Osozawa et al. (2019).

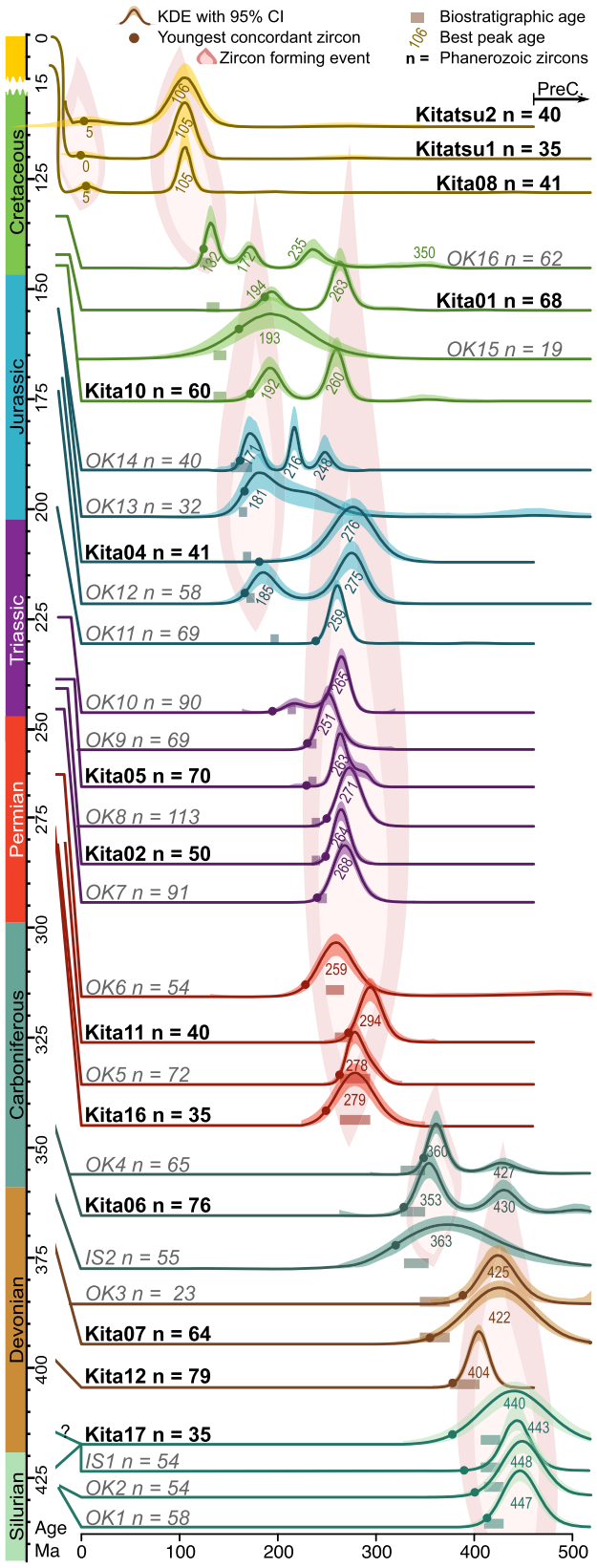

Fig. 3. Zircon spectra in the Kita (new dataset), OK (Okawa et al., 2013) and IS (Isozaki et al., 2014) samples from the South Kitakami forearc basin.

Permian-Mesozoic samples, which have no or negligible amounts of pre-Permian zircon; and Cenozoic samples, whose spectra display no zircon older than ~120 Ma.

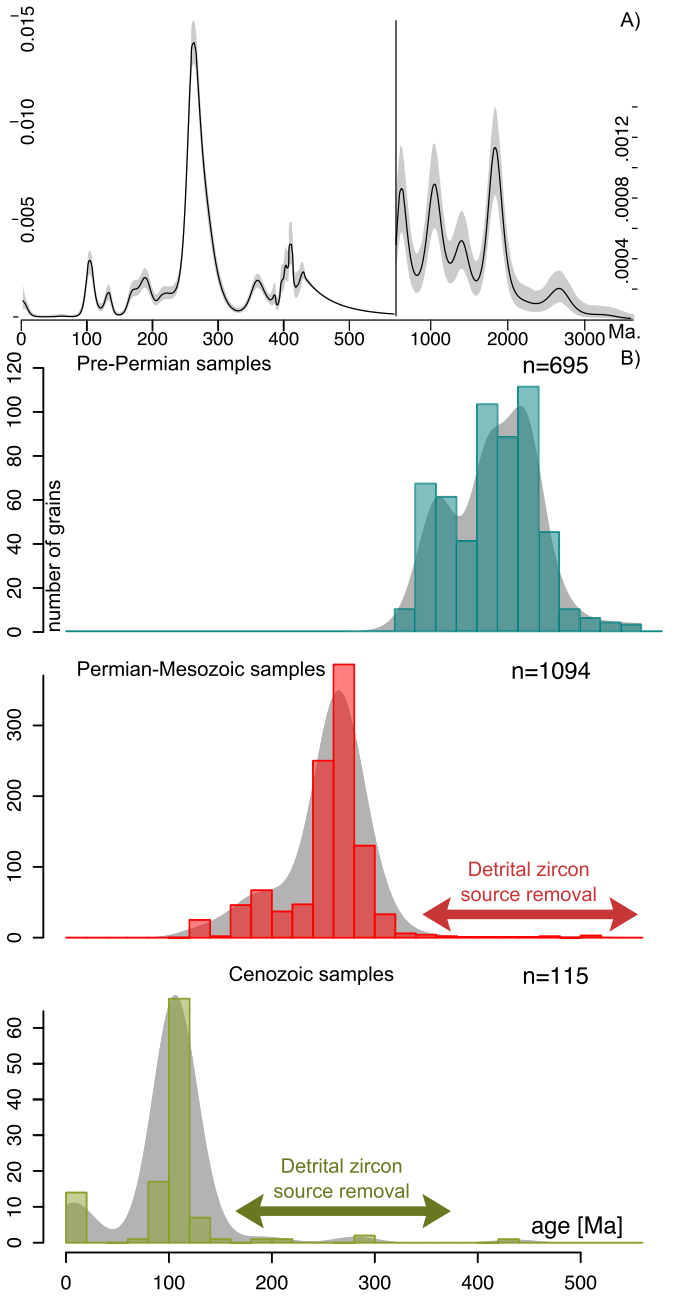

Fig. 4. A) Composite spectra of all detrital samples. B) Composite spectra of all pre-Permian samples. C) Composite spectra of the Permian-Mesozoic samples. D) Spectra of the three Cenozoic samples studied.

A composite age spectrum of all detrital samples defines the synthetic dominant zircon population for SKFB (Fig. 4). The number of pre-Cambrian zircon is residual (n = 190, 11%), none of the peaks is statistically relevant. If we consider only the total Precambrian zircon, 3 peaks are significant: ~0.6 Ga, 1 Ga, and 1.9 Ga. We identified 6 synthetic dominant zircon populations at 430 ± 20, 360 ± 10, 270 ± 20, 184 ± 12, 112 ± 22, and 7 ± 7 Ma. We have plotted all individual samples in a multi-dimensional scaling (MDS) map (Vermeesch, 2013) against and the synthetic zircon population ages (Fig. 5; Spencer and Kirkland, 2016). MDS transforms a matrix of pairwise similarities (the D value from the Kolmogorov-Smirnov test) into a cartesian two-dimensional space showing all detrital zircon populations considered. On a MDS diagram distances represent the degree of similarity, the smaller the distance between two samples the more similar they are (Ver-

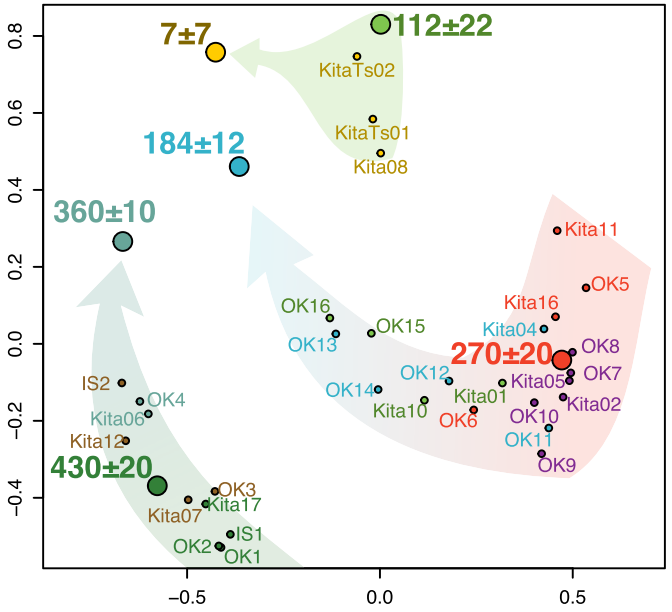

Fig. 5. Multidimensional Scaling map of all detrital zircon samples depicting the similarities and evolution of the three identified groups based on the total loss of the previous distributions (pre-Permian, Permian-Mesozoic and Cenozoic).

meesch, 2013). The plot is dimensionless and values range between 0, and 1 on each axis. A distance of 0 between two samples means a perfect match and 1, no overlap between two distributions). The MDS map displays three clusters: the Pre-Permian samples; the Permo-Mesozoic samples and the Cenozoic samples.

The $^{176}Hf/^{177}Hf$ isotopic signature in zircon represents a proxy to estimate when the rock that crystallized such zircon was extracted from the mantle and to diagnose crustal reworking through time, where successive samples define a Hf evolution array (e.g. Spencer et al., 2019). Hf isotopic analyses of Hikami samples (Kita13 and OSO-08) have initial εHf values of −10 to +1 (Fig. 6A). The εHf values for the SKM Cretaceous granitoids (OSO-01 to 07) vary from 5 to 13, although other Tohoku areas (see Osozawa et al., 2019) exhibit a wider range (from −20 to 15), being from 0 to 15 the most concentrated area (Fig. 6A). Precambrian zircon show very variable εHf signatures, ranging from −20 to positive values close to the depleted mantle curve (Fig. 6B). No zircon older than 1.5 Ga has positive values. The Phanerozoic detrital zircon Hf evolution through the stratigraphy shows an εHf increase from ∼430 Ma, with initial εHf values very similar to those of Hikami granite, to ∼360 Ma where εHf values range from ∼0 to ∼10. From ∼360 Ma, εHf trend increases with a less pronounced slope but losing all the less juvenile sources to ∼270 Ma, where values get close to the depleted mantle curve. From there εHf decreases until ∼112 Ma following a typical crustal residence trend. At around 112 Ma detrital zircon register, as in the igneous rocks, values ranging from quite positive to about 0, mimicking the Cretaceous granitoids trend. The Hf-isotope array displays a similar effect in the sub recent population of zircon (Fig. 6B).

4. Discussion

The new samples (Kita) and reappraised (OK, IS and OSO samples from Okawa et al., 2013; Isozaki et al., 2014 and Osozawa et al., 2019, respectively) provide a crucial source of information to understand the Phanerozoic crustal history of Japan. The detrital zircon spectra through the stratigraphic column of SKFB revealed that most samples present unimodal or bimodal age peaks; younging upwards maximum depositional ages comparable to their biostratigraphic ages; and with minor to no Precambrian contribution (Figs. 3 and 6). A synthetic detrital zircon spectrum considering all new and literature samples from SKM has 6 statistically significant populations at 430 ± 20, 360 ± 10, 270 ± 20, 184 ± 12, 112 ± 22, and 7 ± 7 Ma (Figs. 3, 4 and 5). All samples but Orikabetoge Formation (Kita17 and IS1) showed maximum depositional ages in line with the biostratigraphic age (Figs. 2 and 3). The youngest concordant zircon from formation are significatively younger than its published biostratigraphic age (∼30 m.yrs). Its zircon distribution is, nonetheless, very similar to the other Silurian units. Both samples were collected in the same area (Fig. 2). Published literature mentions the lithological similarities between Silurian and Devonian clastic rocks in that area and geologic relationships are often obscured by minimal rock exposure (Ehiro et al., 2016). Therefore, we cannot rule out that samples were collected in a Devonian unit.

4.1. Provenance of the South Kitakami forearc

The sedimentary system of the Japanese forearc in SKM experienced limited sedimentary reworking of older forearc material and little sediment support from cratonic and orogenic areas located to the west (present-day coordinates). The major peaks in each sample (Fig. 3; Okawa et al., 2013; Isozaki et al., 2014) deviate very little from the dominant synthetic zircon age populations (430 ± 20, 360 ± 10, 270 ± 20, 184 ± 12, 112 ± 22, and 7 ± 7 Ma). Additionally, samples fall into three categories defined by the range of dominant zircon age populations (Fig. 4) pre-Permian, Permian-Mesozoic, and Cenozoic. The zircon support to the basin is controlled therefore by several detrital zircon forming events (coincident with the synthetic populations) and by two major time boundaries (late Carboniferous-early Permian and late Cretaceous) when the older arc and forearc stopped supporting zircon to the basin.

The paucity of Precambrian zircon (190/1991, ∼10%) indicates that the volcanic arc has acted as a long-term barrier impending transport of zircon from any craton. The combined Precambrian age spectra show three main populations (Fig. 6B) at ∼600, ∼1000, and 1900 Ma, and two minor peaks at ∼1500 and ∼2800 Ma, which are consistent with a minor inflow of sediment to the forearc basin from South China Craton where the proto-Japan arc was likely located until the Triassic (Isozaki, 2019). So far, the 1900 Ma peak has not occurred in NE Gondwana, and the ∼1000 Ma one is largely absent in North China (e.g. Zhao et al., 2017). The disappearance of Precambrian zircon during the Permian–Triassic times and reappearance in the SKM record from the Jurassic might be indicative of the Permo-Triassic collisional events in east-central China (e.g. Isozaki, 1997; Ernst et al., 2007) and its sedimentary dynamics, we cannot reject minor contributions from North China from after such collision.

Despite the SKFB preserves an almost continuous stratigraphy from Silurian to Cretaceous, the prospective pre-Cretaceous arc-related sources of zircon to the basin are generally lacking. Apart from some tuffs intercalated in the pre-Permian stratigraphy (SF1), plutonic rocks older than Cretaceous are extremely scarce in SKM in particular and Japan in general (Fig. 1). In the SKM, the Silurian Hikami Granite (and equivalent plutons not cropping out) could represent the main source for the 430 ± 20 population. The only preserved putative sources for the 360 ± 10 population are minor tuffs (Fig. 2; SF1). No sources for 270 ± 20 and 184 ± 12 Ma populations have been identified so far in SK, being the nearest in age and location the Carboniferous-Permian Wariyama granite in the Abukuma Mountains, to the south (∼300 Ma., Tsutsumi et al., 2010; Tsuchiya et al., 2014). The Permian zircon population is the most prominent not only in SK, but also in other in other Permo-Mesozoic forearc basins and accretionary complexes in SW Japan (e.g. Isozaki et al., 2010; Zhang et al., 2019). However, Permian ig-

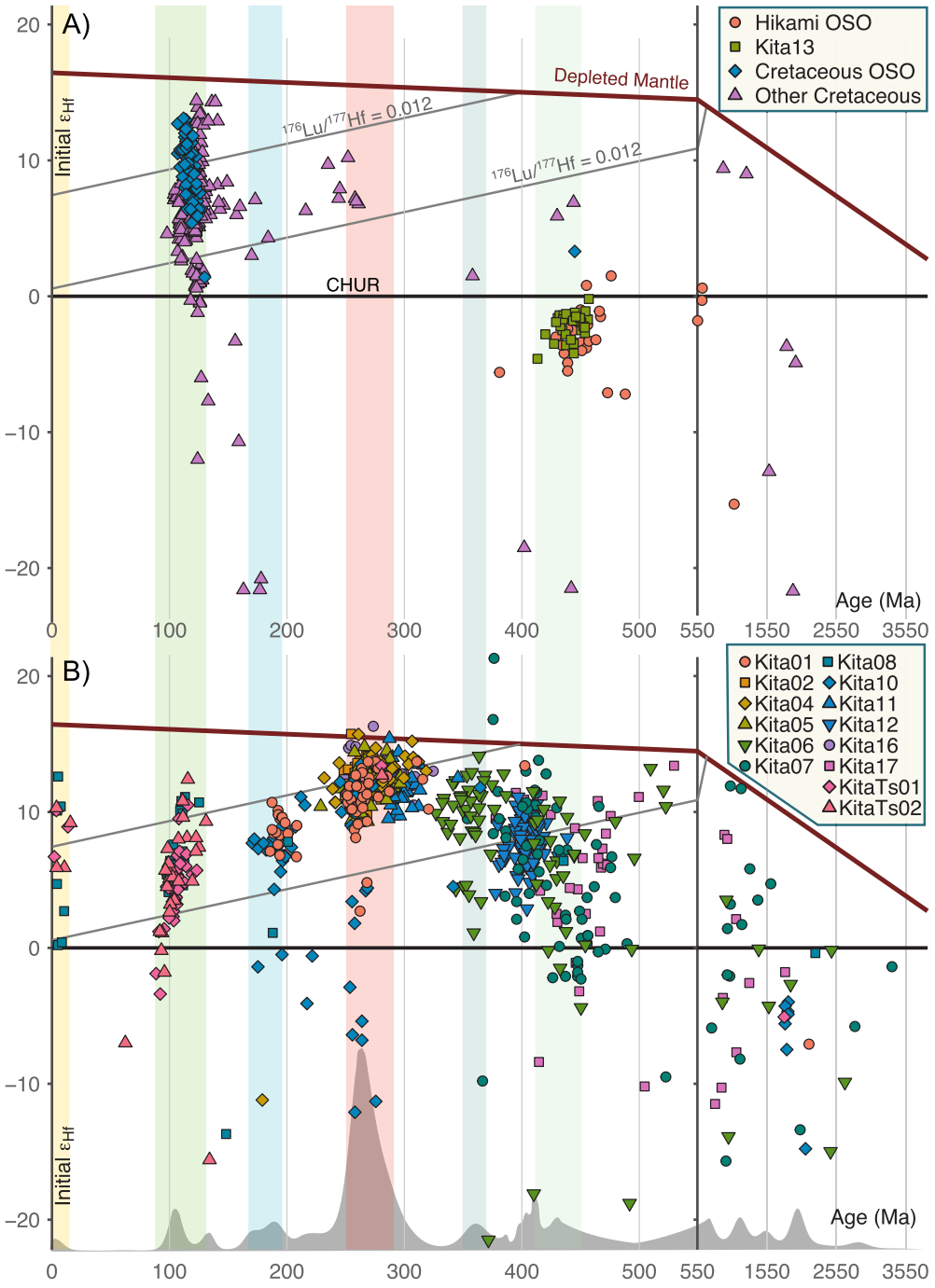

Fig. 6. A) εHf in zircon respect to their U-Pb zircon age for the Hikami Granite (Silurian) and the Cretaceous granitoids of South Kitakami and surroundings (from Osozawa et al., 2019) B) εHf in the detrital zircon vs. their ages (Kita samples).

neous rocks are almost absent in the Japanese record excepting the Hida Belt. In contrast, Miocene to recent andesites and rhyolitic flows and, especially, Cretaceous large batholiths abound in all the Japanese archipelago (Figs. 1 and 2).

4.2. Hf isotopes: Japan sinks, Japan melts

The Precambrian population of zircon in Kita samples is too scarce (n = 49) to interpret important trends in the crustal residence of the source areas. Nonetheless, we think it is a useful preliminary constraint into the contested proto-Japan paleogeography (South China vs. North China, e.g. Isozaki, 2019; Wakita et al., 2021). We distinguished two groups in the Kita samples Hf-isotope array (Fig. 6B). Zircon of the ~1.9 Ga population and older show variable negative values of εHf. The younger populations (~1 Ga and ~600 Ma) have very mixed values, from very positive to negative, suggesting a mixing between significant amounts of newly extracted from the mantle material and other crustal sources. Our Precambrian results are compatible with a provenance from Cathaysia and/or Yangtze blocks (South China craton, Fig. 1), with similar detrital zircon populations and εHf array (Cawood et al., 2018; Wan et al., 2019). In contrast, North China's 1.9 Ga population has quite positive εHf values (Xia et al., 2008). Further data is necessary to confirm such affinity, but with the present dataset, we are inclined towards a proto-Japan arc being part of a Greater South China continent (Isozaki et al., 2014, 2015).

The evolution of Hf-isotope in the Phanerozoic zircon through the stratigraphy (Fig. 6) shows a Hf-isotope array that starts with similar values to the Hikami granite (Kita 13 and OSO 08 from Osozawa et al., 2019). The age similarity and εHf signature suggest that Hikami and/or very similar non-preserved Silurian plutons fed the forearc basin during the Silurian-Carboniferous times. The εHf/Ma trend displays progressively more juvenile (positive) values as the zircon population gets younger. This indicates that the sources of Devonian and Early Carboniferous zircon mixed depleted mantle material with the previous SKM crust. From ~360 Ma, the trajectory keeps on increasing until ~270 Ma with very positive values in the proximity of the depleted mantle curve. Remarkably, the trend from 360 to 270 Ma loses most of the less juvenile contribution, indicating little crustal mixing of the sources of Carboniferous and Permian zircon. We interpret that the steep εHf/Ma trajectory from 450 to 270 Ma implies a progressive loss of the original proto-Japan crust. At the beginning of such a process (from ~450 to ~360 Ma) the growing contribution in the SK crust from the depleted mantle was mixing with the previous crust. From ~360 to ~270 Ma less crustal mixing occurred, indicating an almost complete loss of the previous crust during the Late Paleozoic. This process ended with a complete crustal replacement in the Permian.

From ~270 Ma, εHf trend decreases until ~112 Ma following a typical crustal residence trend. We interpret the trend as a period in which the Permian new crust matured and where, despite the Jurassic minor flare-up, new mantle input was minor. At around 112 Ma detrital zircon register, analog to the igneous rocks, values ranging from quite positive to about 0, the same as in the sub recent population of zircon (Fig. 6B). It indicates a lot of mixing between the Permian crust and new inputs from the depleted mantle. Considering that the majority of the present-day Japan arc crust is a Cretaceous large batholith, we support that the majority of the Japanese crust melted during a punctual and diachronic event (in Tohoku ~112 Ma, progressively younger to the South and west, Osozawa et al., 2019). Some authors attributed the magmatic event to the subduction of the Izanagi plate's ridge below Japan (e.g. Maruyama and Seno, 1986; Maruyama et al., 1997), although the kinematics, timing, and orientation of the ridge subduction are disputed (see Wu and Wu, 2019 for discussion and references).

The gap in the SKFB zircon record from the Cretaceous population to the recent population hinders the crustal evolution during the Late Cretaceous and Paleogene. Other fragments of the forearc basin like the Izumi Group in SW Japan) may shed light on the crustal evolution since samples generally show unimodal detrital zircon peak at ~80 Ma, however, Hf-isotope signatures have not been studied so far (Aoki et al., 2012). The sub-recent population shows a range of juvenile εHf (from ~0 to ~12). This indicates, again, the mixing of new depleted mantle sources and former crust. In this case, we think that the retreat of the arc after the Miocene opening of the Japan Sea (Van Horne et al., 2017 and references therein) explains best the Miocene to recent Hf-isotope trend.

4.3. Flaring up and dragging Japan down

The Phanerozoic zircon pool of individual sample spectra shows dominant populations that are roughly coeval and little Precambrian zircon sources (Fig. 3). The dominant populations, confirmed by the composite Phanerozoic detrital zircon spectra of SKFB (1801 out of 1991 zircon), are late Silurian, early Carboniferous, Permian, early Jurassic, Aptian-Albian, and sub-recent in age. The youngest population in each spectrum does not get progressively younger as we go upwards in the stratigraphy (Fig. 3), or not to a significant level. For example, OK6 (Permian strata) has a younger peak than all Triassic samples whose youngest peak is Permian but one. Older populations get progressively less important, to finally disappear forever (Fig. 3). In addition to the progressive loss of previous sources, both the individual and the composite spectra evince that Post-Carboniferous samples do not display any pre-Permian zircon age peaks (Figs. 3 and 4). Likewise, Cenozoic samples do not show any pre-Cretaceous zircon age peaks (Figs. 3 and 4). This leaves three groups (Pre-Permian, Permian-Mesozoic, and Cenozoic, Fig. 4) that are further justified by the use of MDS by comparing the SKFB samples with synthetic age populations (Fig. 5). In the MDS map, the Pre-Permian samples cluster near the early Silurian population with a trend as samples go upwards in the column towards the early Carboniferous. Following a similar pattern, the Permian-Cretaceous samples cluster near the ~270 $\pm$ 20 Ma synthetic population with a trend towards the Jurassic maxima (184 $\pm$ 12 Ma). Finally, the Cenozoic samples cluster near the ~112 $\pm$ 22 Ma but not far from the 7 $\pm$ 7 Ma population. The Hf-isotope array indicates that the process responsible for the two main events where previous sources disappear could not be the same.

SKFB contains an almost continuous forearc stratigraphy from late Silurian to early Cretaceous (Fig. 2), and most of other geological evidence in the archipelago points to an uninterrupted subduction below Japan during, at least, 400 m.yr (e.g. Maruyama et al., 1997; Isozaki et al., 2010). If arc activity had been continuous and approximately at a constant rate, we would have found a progressively younger maximum depositional age pointing to a progressively younger arc source feeding the basin. However, we found an age consistency of the dominant populations through the stratigraphy, suggesting that significant zircon forming events in the arc were followed by relatively still periods with lesser magmatism. We propose that the main populations represent magmatic flare-ups. Some of these hypothesized flare-ups to occur coeval to main HP-LT metamorphic events (Fig. 1): (1) Silurian – Fuko Pass; (2) early Carboniferous – Renge; and (3) the most obvious, Cretaceous – Sanbagawa, where Cretaceous batholiths paired with coeval HP-LT. The cyclic HP-LT metamorphic together with coeval LP-HT metamorphism and anatexis (Miyashiro's 'paired metamorphic belt' concept (1961)) are common in long-lived Pacific type orogeny (e.g. western USA: Snoke and Barnes, 2006) and potentially related to flare-ups. The only tectonic events close to coeval to the Permian maxima is the collision of Maizuru arc and the subrecent population fits in time with the opening of the Japan Sea (Fig. 1). We could not find any event that can explain the Jurassic zircon maxima.

The progressive depletion of older populations upwards in the stratigraphy indicates the loss of the igneous source and little reworking of previous strata. Low rates of basin reworking suggest protracted subsidence keeping the basin away from erosion. The fading of the older zircon sources may be related to its burial below newer arc material; high erosion rates enough to completely erode the source rocks; or tectonic erosion removing the oldest section of the arc from below. Complete burial would require continuous arc production. Our zircon record evidences intermittent magmatic flare-ups instead. Large amounts of magmatism during a flare-up could be blamed for the burial of older sources. In such a case, it would be expected that these older sources became more present after several million years of erosion of the flare-up, but we found the opposite. The complete erosion of previous arcs manifests similar setbacks: if the arc had been repeatedly dismantled due to high erosion rates, we would have found Precambrian zircon coming from the cratons each time the arc did not represent a sedimentary barrier. Previous studies (e.g. Suzuki et al., 2010; Isozaki et al., 2010) suggested that the Japan arc has undergone frequent periods of tectonic erosion since the Silurian, removing significant parts of its geological record. Tectonic erosion (von Huene and Lallemand, 1990) can explain both the disappearance

of older arc sources, the mixing of Hf-isotope signatures becoming progressively more juvenile, and continuous subsidence of the forearc.

Nonetheless, the main two events when the older sources completely disappeared (Late Carboniferous - Early Permian and Cretaceous) are hardly explained by tectonic erosion. During the late Carboniferous event, the Hf-isotope array shows the arc crust was completely renewed (Fig. 6B). Delamination of the lithospheric mantle (e.g. Magni and Király, 2020) can explain the partial removal of the lower crust and the generation of mantle-derived magmatism, whereas the consequent uplift produces rapid and intense denudation. We think this is the most plausible mechanism explaining the quick removal of the Precambrian crust in NE Japan and the subsequent Permian flare-up (Figs. 3 and 6B). Candidates triggering delamination in the overriding plate are a rapid arc retreat, for example, due to slab roll-back, or collision of an arc or oceanic plateau that stagnated below Japan, resulting in an overthickened crust and forming a convective drip at the base of the thickened lithosphere. So far, we have not been able to find compelling evidence of late Carboniferous widespread extension and development of large back-arc in the Japanese and East Asia margin (e.g. Shen et al., 2018). In contrast, the only collisional candidate (Maizuru; Fig. 1) is too young and it is uncertain whether the magnitude of the collision was enough to precipitate a delamination event (Fig. 1, Isozaki et al., 2010). The Hf-isotope signature of the Cretaceous zircon sources loss event suggests, in contrast to the late Carboniferous, a general mixing between the older and the juvenile crust. The crustal reworking time is coeval to the emplacement of the Cretaceous batholiths with frequent adakitic composition (Tsuchiya et al., 2014; Osozawa et al., 2019) that represents the bulk of today Japanese crust, and the final subduction of the Izanagi plate (c.f. Wu and Wu, 2019). We found appealing a cause-effect relationship between the final subduction of the Izanagi ridge, the formation of slab windows, and the development of a flare-up that adds new material from the depleted mantle and was capable of melting the majority of the Permian crust of Japan. We also think that the Miocene opening of the Japan Sea explains well the character of the sub-recent zircon population. The detrital zircon of SKFB tell us the hidden history of the missing record of Japan, a violent tale of flare-ups, crustal melting, and lithospheric foundering.

5. Conclusions

The composite Phanerozoic detrital zircon spectra of the SKFB of Japan define dominant zircon age populations at ~430, ~360, ~270, ~180, ~112, and ~7 Ma. We found very few Precambrian zircon, which indicate the arc acted as a barrier for craton support during all Phanerozoic. In addition to these dominant populations, we recognize a progressive disappearance of older sources and three distinct time intervals with very few to no zircon: ~320 to 300 Ma; ~160 to 140 Ma and ~60 to 20 Ma. These gaps are coincident with tectonically quiescence periods in Japanese magmatism. The $^{176}Hf/^{177}Hf$ isotopic signature of the zircon spectra shows an εHf increase from ~430 Ma to ~270 Ma when the Japanese crust became completely juvenile. From there εHf decreases until ~112 Ma following a typical crustal residence trend. At around 112 Ma detrital a quick event mixed the Permian crust with new input from the mantle. We found a similar effect in the sub recent population of zircon.

The SKFB detrital zircon record evinces a geological history punctuated by magmatic flare-ups, which produced large amounts of zircon, and periods with very little arc activity. The progressive disappearance of older sources of zircon reveals a protracted ~500 m.yr. of tectonic erosion, which hindered the crustal growth in Japanese arc. Finally, Hf isotopes revealed two catastrophic events: A late Carboniferous loss of the Japanese crust, which we interpret as a delamination process, and a Cretaceous melting of the entire arc, probably related to the subduction of the mid-oceanic ridge separating the Izanagi and Pacific plates.

CRediT authorship contribution statement

Daniel Pastor-Galán: Conceptualization, Validation, Formal Analysis, Resources, Investigation, Visualization, Data Curation, Writing, Funding Acquisition.

Christopher J. Spencer: Conceptualization, Methodology, Formal Analysis, Investigation, Visualization, Data Curation, Writing-review and editing, Funding Acquisition.

Tan Furukawa: Software, Formal Analysis, Visualization, Resources.

Tatsuki Tsujimori: Validation, Writing-review and editing, Funding Acquisition.

Declaration of competing interest

The authors declare that they have no known competing financial interests or personal relationships that could have appeared to influence the work reported in this paper.

Acknowledgements

We would like to thank Xiaofang He, Brad McDonald, and Noreen Evans for lab assistance. Hiroyuki Okawa and Soichi Osozawa kindly provided their datasets to be included in this paper. Research in the GeoHistory laser ablation Facility, John de Laeter Centre, Curtin University of Technology is supported by AuScope (auscope.org.au) and the Australian Government via the National Collaborative Research Infrastructure Strategy (NCRIS). The NPII multi-collector was obtained via funding from the Australian Research Council LIEF program (LE150100013). The constructive comments by Yukio Isozaki and an anonymous reviewer greatly improved the paper. This paper was funded by MEXT/JSPS KAKENHI Grant (JP15H05212, JP16F16329, JP18H01299) and an "Ensemble Grant for Young Researchers" (Tohoku University). DPG also thanks a lifetime of company provided by Christopher John Cornell. You broke your rusty cage, now the cold Earth is your bed.

Appendix A. Supplementary material

Supplementary material related to this article can be found online at https://doi.org/10.1016/j.epsl.2021.116893. These data include the Google map of the most important areas described in this article.

References

Aoki, K., Isozaki, Y., Yamamoto, S., Maki, K., Yokoyama, T., Hirata, T., 2012. Tectonic erosion in a Pacific-type orogen: detrital zircon response to Cretaceous tectonics in Japan. Geology 40, 1087–1090. https://doi.org/10.1130/G33414.1.

Bouvier, A., Vervoort, J.D., Patchett, P.J., 2008. The Lu-Hf and Sm-Nd isotopic composition of CHUR: constraints from unequilibrated chondrites and implications for the bulk composition of terrestrial planets. Earth Planet. Sci. Lett. 273, 48–57. https://doi.org/10.1016/j.epsl.2008.06.010.

Cawood, P.A., 2005. Terra Australis Orogen: Rodinia breakup and development of the Pacific and Iapetus margins of Gondwana during the Neoproterozoic and Paleozoic. Earth-Sci. Rev. 69 (3–4), 249–279.

Cawood, P.A., Zhao, G., Yao, J., Wang, W., Xu, Y., Wang, Y., 2018. Reconstructing South China in Phanerozoic and Precambrian supercontinents. Earth-Sci. Rev. 186, 173–194. https://doi.org/10.1016/j.earscirev.2017.06.001.

Ehiro, M., Tsujimori, T., Tsukada, K., Nuramkhaan, M., 2016. Palaeozoic basement and associated cover. In: Moreno, T., et al. (Eds.), The Geology of Japan: Bath. Geological Society Publishing House, pp. 25–60.

Ernst, W.G., Tsujimori, T., Zhang, R., Liou, J.G., 2007. Permo-Triassic collision, subduction-zone metamorphism, and tectonic exhumation along the East Asian continental margin. Annu. Rev. Earth Planet. Sci. 35, 73–110. https://doi.org/10.1146/annurev.earth.35.031306.140146.

Geological Survey of Japan, AIST (ed.). 2021. Seamless digital geological map of Japan 1: 200,000 V2. January 22, 2021 version. Geological Survey of Japan, AIST. https://gbank.gsj.jp/seamless/index_en.html.

Griffin, W.L., Pearson, N.J., Belousova, E., Jackson, S.E., van Achterbergh, E., O'Reilly, S.Y., Shee, S.R., 2000. The Hf isotope composition of cratonic mantle: LAM-MC-ICPMS analysis of zircon megacrysts in kimberlites. Geochim. Cosmochim. Acta 64, 133–147. https://doi.org/10.1016/S0016-7037(99)00343-9.

Harada, H., Tsujimori, T., Kunugiza, K., Yamashita, K., Aoki, S., Aoki, K., Takayanagi, H., Iryu, Y., 2021. The $\delta^{13}C$ -$\delta^{18}O$ variations in marble in the Hida Belt, Japan. Isl. Arc 30, e12389.

Ishiwatari, A., Tsujimori, T., 2003. Paleozoic ophiolites and blueschists in Japan and Russian Primorye in the tectonic framework of East Asia: a synthesis. Isl. Arc 12, 190–206. https://doi.org/10.1046/j.1440-1738.2003.00390.x.

Isozaki, Y., 2019. A visage of early Paleozoic Japan: geotectonic and paleobiogeographical significance of Greater South China. Isl. Arc 28, e12296. https://doi.org/10.1111/iar.12296.

Isozaki, Y., 1997. Contrasting two types of orogen in Permo-Triassic Japan: accretionary vs. collisional. Isl. Arc 6, 2–24. https://doi.org/10.1111/j.1440-1738.1997.tb00038.x.

Isozaki, Y., Aoki, K., Nakama, T., Yanai, S., 2010. New insight into a subduction-related orogen: a reappraisal of the geotectonic framework and evolution of the Japanese Islands. Gondwana Res. 18, 82–105. https://doi.org/10.1016/j.gr.2010.02.015.

Isozaki, Y., Aoki, K., Sakata, S., Hirata, T., 2014. The eastern extension of Paleozoic South China in NE Japan evidenced by detrital zircon. GFF 136, 116–119. https://doi.org/10.1080/11035897.2014.893254.

Isozaki, Y., Ehiro, M., Nakahata, H., Aoki, K., Sakata, S., Hirata, T., 2015. Cambrian plutonism in Northeast Japan and its significance for the earliest arc-trench system of proto-Japan: new U-Pb zircon ages of the oldest granitoids in the Kitakami and Ou Mountains. J. Asian Earth Sci. 108, 136–149. https://doi.org/10.1016/j.jseaes.2015.04.024.

Ito, T., Kojima, Y., Kodaira, S., Sato, H., Kaneda, Y., Iwasaki, T., Kurashimo, E., Tsumura, N., Fujiwara, A., Miyauchi, T., Hirata, N., Harder, S., Miller, K., Murata, A., Yamakita, S., Onishi, M., Abe, S., Sato, T., Ikawa, T., 2009. Crustal structure of southwest Japan, revealed by the integrated seismic experiment Southwest Japan 2002. Tectonophysics 472, 124–134. https://doi.org/10.1016/j.tecto.2008.05.013.

Jahn, B.M., 2004. The Central Asian Orogenic Belt and growth of the continental crust in the Phanerozoic. Geol. Soc. (Lond.) Spec. Publ. 226, 73–100. https://doi.org/10.1144/GSL.SP.2004.226.01.05.

Magni, V., Király, Á., 2020. Delamination. In: Reference Module in Earth Systems and Environmental Sciences. Elsevier. https://doi.org/10.1016/B978-0-12-409548-9.09515-4.

Maruyama, S., Seno, T., 1986. Orogeny and relative plate motions: example of the Japanese Islands. Tectonophysics 127, 305–329. https://doi.org/10.1016/0040-1951(86)90067-3.

Maruyama, S., Isozaki, Y., Kimura, G., Terabayashi, M., 1997. Paleogeographic maps of the Japanese Islands: plate tectonic synthesis from 750 Ma to the present. Isl. Arc 6, 121–142.

Miyashiro, A., 1961. Evolution of metamorphic belts. J. Petrol. 2, 277–311.

Okawa, H., Shimojo, M., Orihashi, Y., Yamamoto, K., Hirata, T., Sano, S.I., Ishizaki, Y., Kouchi, Y., Yanai, S., Otoh, S., 2013. Detrital zircon geochronology of the Silurian–Lower Cretaceous continuous succession of the South Kitakami belt, northeast Japan. Mem. Fukui Prefect. Dinosaur Mus. 12, 35–78. https://dl.ndl.go.jp/info:ndljp/pid/10970636.

Osozawa, S., Usuki, T., Usuki, M., Wakabayashi, J., Jahn, B., 2019. Trace elemental and Sr-Nd-Hf isotopic compositions, and U-Pb ages for the Kitakami adakitic plutons: insights into interactions with the early Cretaceous TRT triple junction offshore Japan. J. Asian Earth Sci. 184, 103968. https://doi.org/10.1016/j.jseaes.2019.103968.

Otoh, S., Yamakita, S., Yanai, S., 1990. Origin of the Chichibu Sea, Japan: Middle Paleozoic to Early Mesozoic plate construction in the northern margin of the Gondwana Continent. Tectonics 9 (3), 423–440.

Ozawa, K., Maekawa, H., Shibata, K., Asahara, Y., Yoshikawa, M., 2015. Evolution processes of Ordovician–Devonian arc system in the South-Kitakami Massif and its relevance to the Ordovician ophiolite pulse. Isl. Arc 24, 73–118. https://doi.org/10.1111/iar.12100.

Pastor-Galán, D., Nance, R.D., Murphy, J.B., Spencer, C.J., 2019. Supercontinents: myths, mysteries, and milestones. Geol. Soc. (Lond.) Spec. Publ. 470, 39–64. https://doi.org/10.1144/SP470.16.

Scherer, E., Münker, C., Mezger, K., 2001. Calibration of the Lutetium-Hafnium Clock. Science 293, 683–687. https://doi.org/10.1126/science.1061372.

Shen, L., Yu, J.H., O'Reilly, S.Y., Griffin, W.L., 2018. Tectonic switching of southeast China in the Late Paleozoic. J. Geophys. Res., Solid Earth 123 (10), 8508–8526.

Shimojo, M., Otoh, S., Yanai, S., Hirata, T., Maruyama, S., 2010. LA-ICP-MS U-Pb Age of Some Older Rocks of the South Kitakami Belt, Northeast Japan. J. Geogr. 119, 257–269. https://doi.org/10.5026/jgeography.119.257 (in Japanese with an English abstract).

Snoke, A.W., Barnes, C.G., 2006. Geological Studies in the Klamath Mountains Province, California and Oregon: A Volume in Honor of William P. Irwin. GSA Special Paper, vol. 410. 505 p. https://doi.org/10.1130/SPE410.

Spencer, C.J., Kirkland, C.L., Prave, A.R., Strachan, R.A., Pease, V., 2019. Crustal reworking and orogenic styles inferred from zircon Hf isotopes: Proterozoic examples from the North Atlantic region. In: Climate Change Impacts on Environmental Geosciences. Geosci. Front. 10, 417–424. https://doi.org/10.1016/j.gsf.2018.09.008.

Spencer, C.J., Kirkland, C.L., Taylor, R.J.M., 2016. Strategies towards statistically robust interpretations of in situ U–Pb zircon geochronology. Geosci. Front. 7, 581–589. https://doi.org/10.1016/j.gsf.2015.11.006.

Spencer, C.J., Kirkland, C.L., 2016. Visualizing the sedimentary response through the orogenic cycle: a multidimensional scaling approach. Lithosphere 8 (1), 29–37.

Spencer, C.J., Roberts, N.M.W., Santosh, M., 2017. Growth, destruction, and preservation of Earth's continental crust. Earth-Sci. Rev. 172, 87–106. https://doi.org/10.1016/j.earscirev.2017.07.013.

Stern, C.R., 2011. Subduction erosion: rates, mechanisms, and its role in arc magmatism and the evolution of the continental crust and mantle. Gondwana Res. 20, 284–308. https://doi.org/10.1016/j.gr.2011.03.006.

Suzuki, K., Maruyama, S., Yamamoto, S., Omori, S., 2010. Have the Japanese Islands grown?: five"Japan"s were born, and four"Japan"s subducted into the mantle. J. Geogr. 119, 1173–1196. https://doi.org/10.5026/jgeography.119.1173 (in Japanese with an English abstract).

Tagiri, M., Dunkley, D.J., Adachi, T., Hiroi, Y., Fanning, C.M., 2011. SHRIMP dating of magmatism in the Hitachi metamorphic terrane, Abukuma Belt, Japan: evidence for a Cambrian volcanic arc. Isl. Arc 20, 259–279. https://doi.org/10.1111/j.1440-1738.2011.00764.x.

Tsuchiya, N., Takeda, T., Tani, K., Adachi, T., Nakano, N., Osanai, Y., Kimura, J.I., 2014. Zircon U–Pb age and its geological significance of late Carboniferous and Early Cretaceous adakitic granites from eastern margin of the Abukuma Mountains, Japan. J. Geol. Soc. Jpn. 120, 37–51. https://doi.org/10.5575/geosoc.2014.0003.

Tsujimori, T., Itaya, T., 1999. Blueschist-facies metamorphism during Paleozoic orogeny in southwestern Japan: Phengite K–Ar ages of blueschist-facies tectonic blocks in a serpentinite melange beneath early Paleozoic Oeyama ophiolite. Isl. Arc 8 (2), 190–205.

Tsujimori, T., 2017. Early Paleozoic jadeitites in Japan: an overview. J. Mineral. Petrol. Sci. 112, 217–226. https://doi.org/10.2465/jmps.170406a.

Tsutsumi, Y., Ohtomo, Y., Horie, K., Nakamura, K.I., Yokoyama, K., 2010. Granitoids with 300 Ma in the Joban coastal region, east of Abukuma Plateau, northeast Japan. J. Mineral. Petrol. Sci. 105, 320–327. https://doi.org/10.2465/jmps.091204.

Uchino, T., 2021. Recognition of an Early Triassic accretionary complex in the Nedamo Belt of the Kitakami Massif, NE Japan: new evidence of correlation with SW Japan. Island Arc 30 (1), 12397.

Van Horne, A., Sato, H., Ishiyama, T., 2017. Evolution of the Sea of Japan back-arc and some unsolved issues. Tectonophysics 710–711, 6–20. https://doi.org/10.1016/j.tecto.2016.08.020.

Vermeesch, P., 2018. IsoplotR: a free and open toolbox for geochronology. Geosci. Front. 9, 1479–1493. https://doi.org/10.1016/j.gsf.2018.04.001.

Vermeesch, P., 2013. Multi-sample comparison of detrital age distributions. Chem. Geol. 341, 140–146. https://doi.org/10.1016/j.chemgeo.2013.01.010.

von Huene, R., Lallemand, S., 1990. Tectonic erosion along the Japan and Peru convergent margins. Geol. Soc. Am. Bull. 102, 704–720. https://doi.org/10.1130/0016-7606(1990)102<0704:TEATJA>2.3.CO;2.

Wakita, K., Nakagawa, T., Sakata, M., Tanaka, N., Oyama, N., 2021. Phanerozoic accretionary history of Japan and the western Pacific margin. Geol. Mag. 158 (1), 13–29.

Wan, Y., Xie, H., Dong, C., Kröner, A., Wilde, S.A., Bai, W., Liu, S., Xie, S., Ma, M., Li, Y., Liu, D., 2019. Hadean to Paleoarchean rocks and zircons in China. In: Van Kranendonk, M.J., Bennett, V.C., Hoffmann, J.E. (Eds.), Earth's Oldest Rocks, second edition. Elsevier, pp. 293–327. Chapter 14.

Wu, T.J., Wu, J., 2019. Izanagi-Pacific ridge subduction revealed by a 56 to 46 Ma magmatic gap along the northeast Asian margin. Geology. https://doi.org/10.1130/G46778.1.

Xia, X., Sun, M., Zhao, G., Wu, F., Xu, P., Zhang, J., He, Y., 2008. Paleoproterozoic crustal growth in the Western Block of the North China Craton: evidence from detrital zircon Hf and whole rock Sr-nd isotopic compositions of the Khondalites from the Jining Complex. Am. J. Sci. 308, 304–327. https://doi.org/10.2475/03.2008.05.

Zhang, X., Takeuchi, M., Lee, H.-Y., 2019. Tracing the origin of Southwest Japan using the Hf isotopic composition of detrital zircons from the Akiyoshi Belt. Terra Nova 31, 11–17. https://doi.org/10.1111/ter.12363.

Zhao, T., Feng, Q., Metcalfe, I., Milan, L.A., Liu, G., Zhang, Z., 2017. Detrital zircon U-Pb-Hf isotopes and provenance of Late Neoproterozoic and Early Paleozoic sediments of the Simao and Baoshan blocks, SW China: implications for Proto-Tethys and Paleo-Tethys evolution and Gondwana reconstruction. Gondwana Res. 51, 193–208. https://doi.org/10.1016/j.gr.2017.07.012.

Supplementary File 1

Evidence for crustal removal, tectonic erosion and flare-ups from the Japanese evolving forearc sediment provenance

Daniel Pastor-Galán[1,2,3], Christopher J. Spencer[4,5], Tan Furukawa[3], Tatsuki Tsujimori[2,3]

[1]Frontier Research Institute for Interdisciplinary Science, Tohoku University, Japan
[2]Center for North East Asian Studies, Tohoku University, 980-8576, 41 Kawauchi, Aoba-ku, Sendai, Miyagi, Japan
[3]Department Earth Science, Tohoku University, Japan
[4]School of Earth and Planetary Sciences, The Institute for Geoscience Research (TIGeR), Curtin University, Perth, Australia
[5]Department of Geological Sciences and Geological Engineering, Queen's University, Kingston, Canada

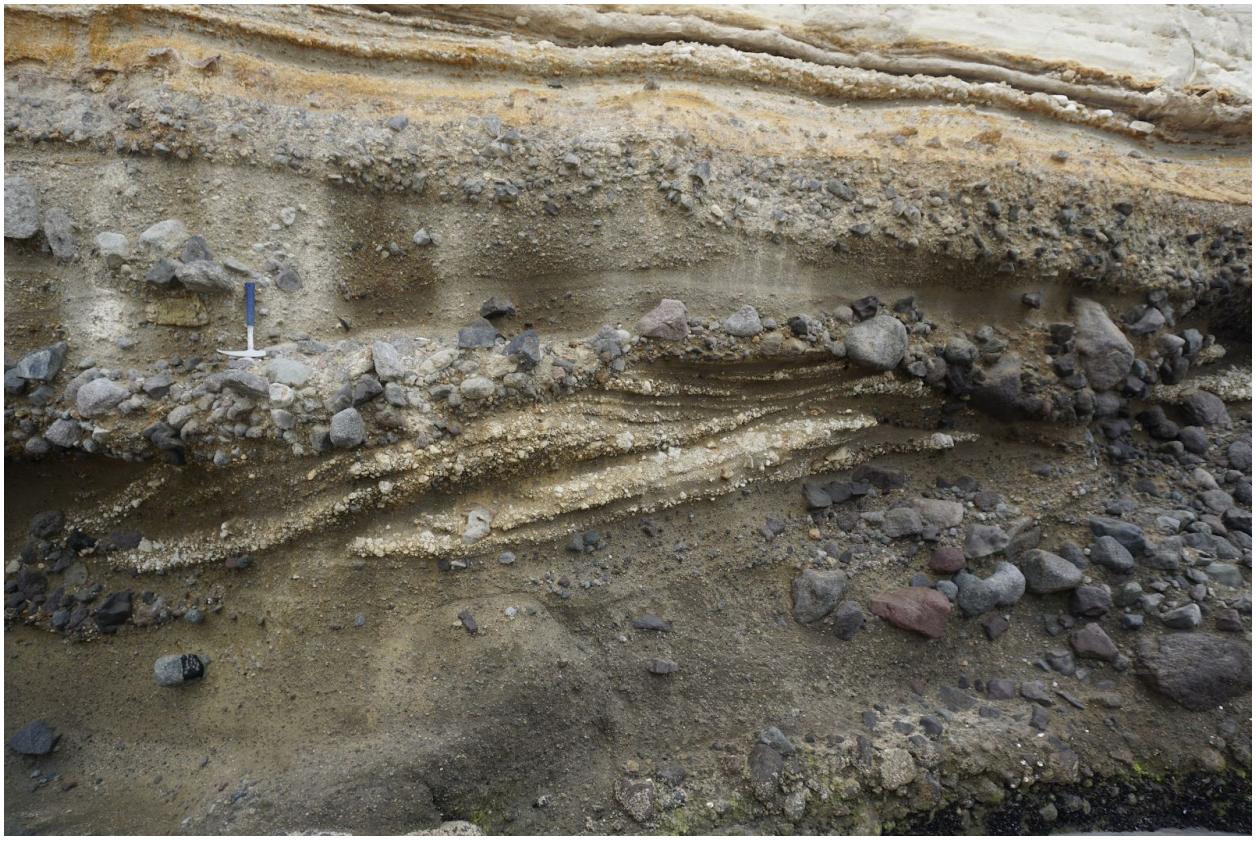

1. Site Description

Here we describe in chronological order, from older to younger, the rock formations sampled in this study (coded Kita) and those coming from the previous papers of Okawa et al. (2013) (re-coded OK) and Osozawa et al. (2019) (re-coded OSO). We provide Osozawa et al.'s (2019) samples and weighted mean ages for each pluton newly coded:

Kita 13: Ordovician-Silurian, Hikami Granite. 39.1008°, 141.6737°

The Hikami Granite is a plutonic body consisting of granites, granodiorites and tonalites. It crops out around Mt Hikami. It is usually unconformably covered by Silurian–Devonian strata. The Hikami granite has recycled zircons of 3000–1300 Ma. The Hikami granite and the Harachiyama volcanics contain chlorite and other secondary minerals, reflecting hydrothermal alteration (Osozawa et al., 2019).

OSO-08: Hikami Granite. 39.1023°, 141.6852°

KTKM-19 wt. mean of most concentrated part = 449.2±4.5 Ma (2σ)
KTKM-20 wt. mean of most concentrated part by grains which Th or U concentration is under 1,000 ppm = 442.4 ± 9.8 Ma (2σ)
BJ-13-107 wt. mean of most concentrated part = 124.9 ± 1.2 Ma (2σ) (Possibly hydrotermally altered, Osozawa et al., 2019)

OK1: Silurian. Nameirizawa Fm. 39.5488°, 141.3389°

OK2: Silurian. Yakushigawa Fm. 39.5352°, 141.6251°

Both formations are equivalent. They start with a tuff and basalts followed by mudstone and sandstone. They contain early Silurian brachiopods (Ehiro et al., 2016).

Kita 17: Silurian (?), Orikabetōge Fm. 39.5246˚, 141.3392˚

The Orikabetōge Formation is composed of conglomerates, arkoses and mudstones with subordinate amounts of limestone and tuff, and a rich fauna of Silurian corals and trilobites (Okami et al. 1986). The conglomerate contains many granitic clasts lithologically similar to Hikami granite.

IS-01 : Silurian (?), Orikabetōge Fm. 39.5286˚, 141.3855˚

Kita 12: Devonian, Ohno Fm. 39.1024˚, 141.6727˚

The Ono Formation is divided into the Oh1, Oh2 and Oh3 members (Minato et al. 1979). The Oh1 Member, which has yielded Pridolian radiolarians (Umeda 1996), is a slump bed which incorporates variously sized clasts of granite, arkose and limestone in a tuffaceous and siliceous mudstone. These clasts are lithologically similar to the underlying Hikami Granite and basal arkose and limestone of the Kawauchi Formation, respectively. The Oh2 Member is composed of acidic tuff and alternating beds of acidic tuff and tuffaceous-siliceous mudstone, and the Oh3 Member similarly consists mainly of tuff with subordinates amount of tuffaceous sandstone and mudstone. We sampled the top section of the formation, with an estimated age of Early-Middle Devonian

Kita 07: Devonian, Tobigamori Fm. 39.0452˚, 141.2509˚

The Tobigamori Formation unconformably overlies the Motai metamorphic complex. It consists of a succession of alternating thick packages of mudstones and thin sandstone beds, with purple tuffs and tuff breccias interbedded in the middle part with a total thickness of ~1000m. Its biostratigraphic age is Famenian (Ehiro and Takaizumi, 1992).

OK3: Devonian. Tobigamori Fm. 39.0672˚, 141.2436˚

IS-02: Carboniferous, Hikoroichi Fm. 39.1297˚, 141.6611˚

The Hikoroichi Formation confomarbly overlies the Devonian sequence and consists of sandstone and limestone. It contains corals, brachiopods and trilobites, and its lower–middle part and upper part are dated as Tournaisian–lower Visean and upper Visean, respectively (Ehiro et al., 2016)

Kita 06: Carboniferous, Karaumedate Fm. 39.0069˚, 141.266˚

Karaumedate formation conformably overlies the Tobigamori Fm. Its depositional age is late Visean. It has very variable thicknesses and it is composed of sandstones and tuffs (Eihiro and Takazumi, 1992)

OK4: Carboniferous. Karaumedate Fm. 39.007˚, 141.2659˚

Kita 16: Permian, Uchikawame Fm. 39.5246˚, 141.2887˚

The Uchikawame Formation is an Early to Middle Permian clastic formation with a thickness between 500 and 1500m. It is composed of mudstones intercalated with thin sandstone and conglomerate beds and lenses (Okami et al., 1986)

OK5: Permian. Nishikori Fm. 38.6873˚, 141.2901˚

It consists of sandstones and mudstones interbeded with minor limestone beds. Its age is Early Permian (Ehiro et al., 2016)

Kita 11: Permian, Hoso Fm. 38.9942˚, 141.5122˚

The Hosoo Formation is dominated by mudstone, and its upper and uppermost parts yield Roadian and Wordian ammonoids, respectively (Ehiro & Misaki 2005).

OK6: Permian Toyoma Fm. 38.8006˚, 141.5511˚

A mudstone with minor intercapations of sandstone. Tha age is Late Permian based on Wuchiapingian ammonoids (Ehiro et al., 2016).

OK7: Triassic. Osawa Fm. 38.5324˚, 141.5340˚

The Triassic rocks unconformably overlie the Paleozoic sequences. The Osawa Formation is composed mainly by calcareous and massive mudstones. It contains minor sandstone and conglomeratic lenses. Its age is Olenkian (Early Triassic).

Kita 02: Triassic, Fukkoshi Fm. 38.4426˚, 141.4641˚

The Fukkoshi Formation consists of sandstones and mudstones of Anisian age (Ehiro et al., 2016).

OK8: Triassic. Fukkoshi Fm. 38.7579˚, 141.5275˚

Kita 05: Triassic, Isatomae Fm. 38.4015°, 141.3683°

The Isatomae Formation lies over the Fukkoshi formation and shows a similar bio-stratigraphic Anisian age. Its 1500 m of thickness consists of silts and mudstones intercalated with thick sandstone beds (Ehiro et al., 2016).

OK9: Triassic. Isatomae Fm. 38.7134°, 141.5239°

OK10: Triassic. Shindate Fm. 38.7092°, 141.5101°

The Shindate Formation lies unconformable over the Isatomae Formation. It is composed of thick sandstones and minor mudstone and rare organic rich mudstone. Its age is Carnian (Okawa et al., 2013).

OK11: Jurassic. Niranohama Fm. 38.6931°, 141.5013°

The Niranohama Formation rests unconformably on the Triassic sedimentary sequences. It consists of sandstone and sandy mudstone and contains Hettangian (earliest Jurassic) ammonoids.

OK12: Jurassic. Aratozaki Fm. 38.6962°, 141.4985°

Unconformably over the Triassic strata, the Aratozaki formation is an arkose with conglomerate and minor mudstone. Its biostratigraphic age is Aalenian (Middle Jurassic) (Ehiro et al., 2016).

Kita 04: Jurassic, Tsukinoura Fm. 38.3816˚, 141.4286˚

Unconformably overlying the Isatomae formation, the Tsukinoura Formation starts with a conglomeratic and sandstone section in its lower part and continues with a monotonous thick mudstone package. The lower part yields Bajocian ammonoids (Ehiro et al., 2016)

OK13: Jurassic. Sodenohama Fm. 38.6730˚, 141.4681˚

Conformably over previous Jurassic strata, it consists of sandstones and mudstones with an Oxfordian–Kimmeridgian ammonoid biostratigraphic (based on Ammonoids). Ehiro et al., 2016).

OK14: Jurassic. Oginohama Fm. 38.3045˚, 141.4972˚

Conformably covering the previous Jurassic strata, it is composed of sandstone with intercalated mudstone and conglomerate. It contains Oxfordian–Tithonian ammonoids (Ehiro et al., 2016)

Kita 10: Cretaceous, Yoshihama Fm. 38.5768°, 141.4534°

It is a quartzitic member of the Jusanhama Group. The group unconformably covers the Jurassic strata Nagao Formation and is mainly composed of massive or bedded, quartzose or arkosic sandstones with intercalated mudstones. Biostratigraphic constraints are uncertain. Given its stratigraphic position above the Nagao Formation, the Jusanhama Group is considered to be Early Cretaceous in age (Ehiro et al., 2016).

OK15: Cretaceous. Yoshihama Fm. 38.5737°, 141.4480°

Kita 01: Cretaceous, Kanayama fm. 38.4387°, 141.3771°

This is an informal member from a small outcrop of sandstones and tufts that overlies the uppermost Jurassic Strata. It is located in the outskirts of Ichinoseki. The sample was taken in a quarry.

OK16: Cretaceous. Ayukawa Fm. 38.2916°, 141.5102°

The Ayukawa Formation conformably covers the Oginohama Formation, consists of arkose and mudstone with rare conglomerate. It contains Early Cretaceous ammonoids.

Cretacous, Kitakami Intrusives

Intrusive plutons of the southern Kitakami zone are generally granitoids with adakitic characteristics, usually associated by smaller gabbroid bodies (Osozawa et al., 2019). Chemically, the Cretaceous igneous rocks of South Kitakami Massif are varied representing a diversity of rock types: from gabbro to syenogranite, from calc-alkalic to calcic. Most of them are magnesian I type graniteoids

We have selected from Osozawa et al. (2019) the U-Pb, Lu-Hf and Sm-Nd data pertaining the plutons of south Kitakami massif:

OSO-01: Cretaceous. Tono Pluton

Tono shows a an adakitic REE pattern with a positive Eu anomaly especially in its central silicic part (Osozawa et al., 2019).
KTKM-04 wt. mean = 118.0±1.2 Ma (2σ)
This sample includes Lu-Hf

OSO-02: Cretaceous. Hitokabe Pluton

Hitokabe has an adatakitic composition.
KTKM-23 wt. mean = 114.4±1.1 Ma (2σ)

OSO-03: Cretaceous. Goyosan Pluton

KTKM-18 wt. mean = 121.7 ± 1.0 Ma (2σ)
KTKM-27 wt. mean = 120.0±2.0 Ma (2σ)
KTKM-28 wt. mean = 125.5±2.4 Ma (2σ)

OSO-04: Cretaceous. Hondera Pluton

KTKM-05 wt. mean = 113.1±1.2 Ma (2σ)

OSO-05: Cretaceous. Orikabe Pluton

This pluton shows a shoshonitic composition.

KTKM-25 wt. mean = 111.5±2.8 Ma (2σ)
KTKM-26 wt. mean = 119.0±1.9 Ma (2σ)

OSO-06: Cretaceous. Kesengawa Pluton

KTKM-21 wt. mean of most concentrated part = 122.1±1.3 Ma (2σ)

OSO-07: Cretaceous. Hirota Pluton

KTKM-22 wt. mean = 121.8±1.1 Ma (2σ)

Kita 08: Miocene, Tatsunokuchi Fm. 39.0448°, 141.2506°

The tatsunokuchi formation consists of sandstones, mudstones and tuffs. The Tatsunokuchi Formation is mainly composed of tidal flat and estuarine deposits (Yoshida et al., 2017).

Kita Tsu: Present Day, Arahama Beach, 38.2185°, 140.9866°

We sampled two differently coloured strata (dark grey and brown in the photo) from Arahama Beach, near Sendai.

2. Extra Figures

Kita 13: Ordovician-Silurian, Hikami Granite. 39.1008°, 141.6737°

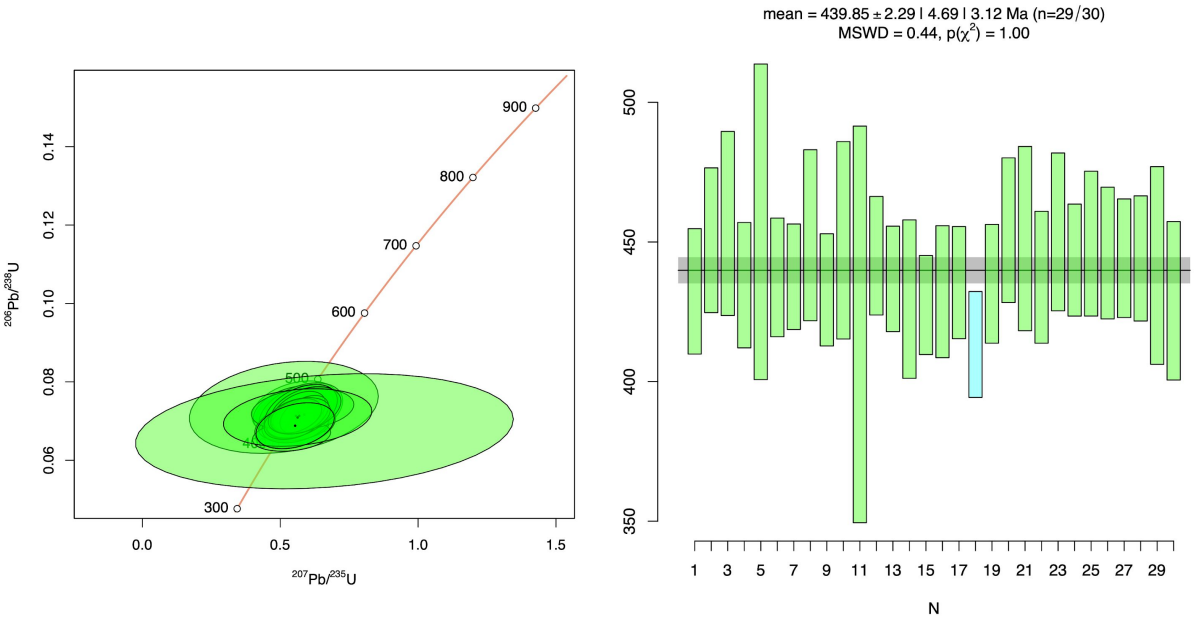

Concordia diagram (left) and mean age for the Kita 13 sample.

Map of the granitoids of Japan

Distribution of granitoids in Japan. The location of the South Kitakami mountains is marked.

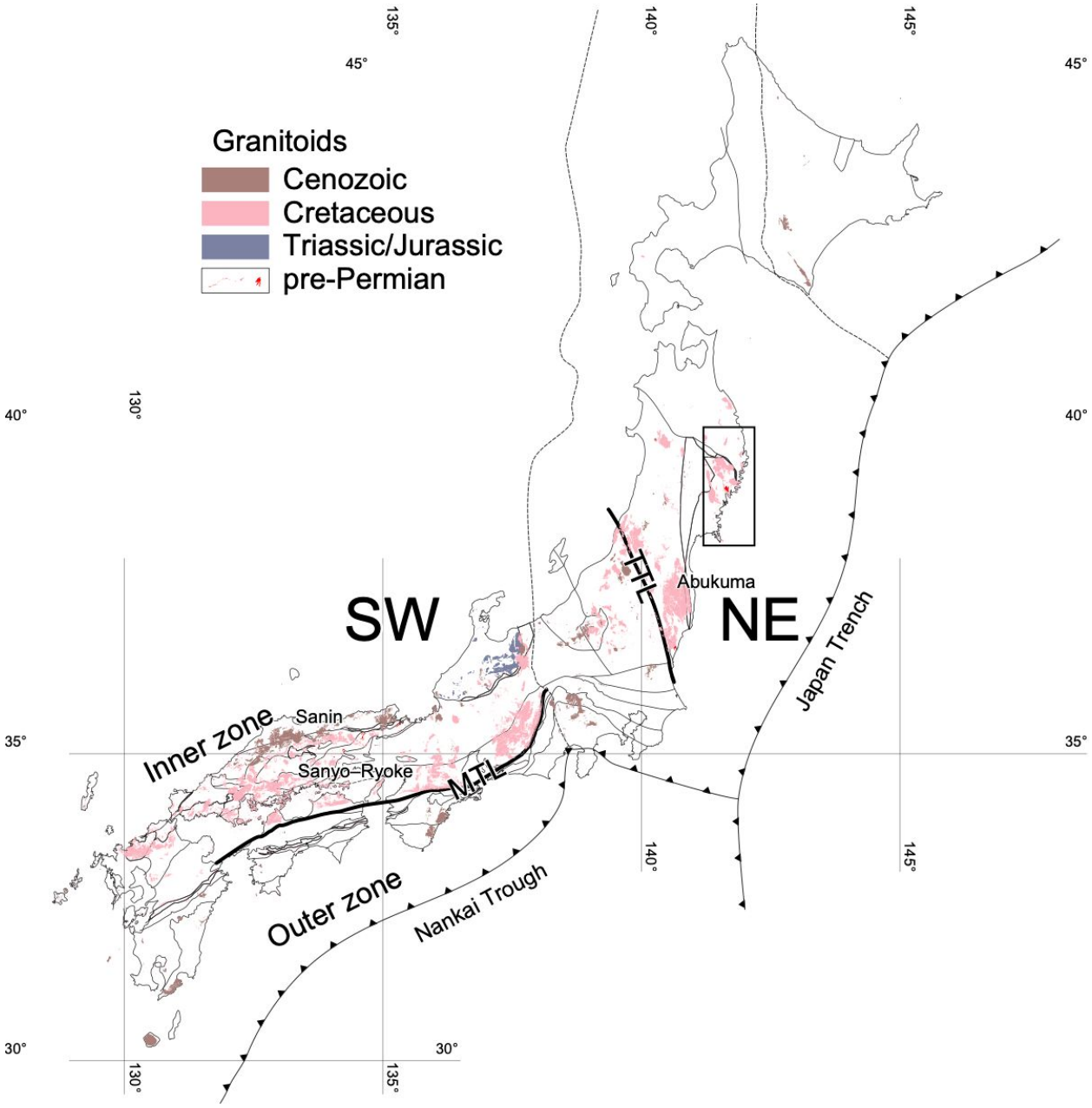

3. BAD-ZUPA

BAD-ZUPA (Bayesian Approach for Detrital Zircon U-Pb ages) is a new evaluation protocol based on Riihimaki and Vehtari (2014)'s Laplace approximation with logistic Gaussian process regression (LA-LGP). BAD-ZUPA evaluates the probability density function (PDF) and their integration, the cumulative distribution function (CDF) through two algorithms: (I) confidence interval estimation and (II) peaks estimation. With BAD-ZUPA, we can evaluate the confidence we have on a detrital zircon spectrum and the significance of the observed peaks. In addition, BAD-ZUPA is a powerful tool to estimate how many more zircons we would need to analyze to obtain a desired level of confidence.

The code is citable though the DOI:

10.5281/zenodo.4138657

The code and a short description and a user manual is available in:

https://github.com/Tan-Furukawa/badzupa

https://rdrr.io/github/Tan-Furukawa/badzupa/

4. Zircon standards used

The primary reference material analyzed for U–Pb dating in this study was 91500 (1,062.4 ± 0.4 Ma in Wiedenbeck et al. (1995) with GJ1 (601.92 ± 0.7 Ma in Jackson et al., 2004) as a secondary age standard. During the two analytical sessions, 91500 yielded a $^{206}Pb/^{238}U$ weighted average age of 1,062 ± 3 Ma (MSWD = 3.6, n = 61; self-normalized) and 1062 ± 2 Ma (MSWD = 0.9, n = 39). GJ1 yielded a $^{206}Pb/^{238}U$ weighted average age of 603 ± 2 Ma (MSWD = 13.5, n = 62) and 601 ± 2 Ma (MSWD = 5.1, n = 40). Ages calculated for the secondary standards, treated as unknowns, were found to be within 1% of the accepted value. The time-resolved mass spectra were reduced using the U_Pb_Geochronology3 data reduction scheme in Iolite (Paton et al., 2011).

Reference zircon Mudtank (0.282507 ± 0.000008 in Fisheret al., 2014) was used to monitor accuracy and precision of internally corrected (using $^{179}Hf/^{177}Hf = 0.7325$) Hf isotope ratios (Woodhead & Hergt, 2005). 91500 (0.282306 ± 0.000008) and GJ1 (0.282000 ± 0.000005 in Morel et al., 2008) were used as secondary standards. During the analytical sessions, Mudtank yielded a corrected $^{176}Hf/^{177}Hf$ weighted average ratio of 0.282507 ± 0.000006 (MSWD = 1.1, n = 62; self-normalized) and 02.28507 ± 0.000006 (MSWD = 1.0, n = 42). 91500 yielded a corrected $^{176}Hf/^{177}Hf$ weighted average ratio of 0.282307 ± 0.000012 (MSWD = 2.2,

n = 61) and 0.282296 ± 0.000008 (MSWD = 1.5, n = 42). GJ1 yielded a corrected 176Hf/177Hf weighted average ratio of 0.282022 ± 0.000010 (MSWD = 2.0, n = 62) and 0.282011 ± 0.000008 (MSWD = 1.7, n = 42). All of the corrected values of secondary standards are within 0.01% of the correct value. The stable $^{178}Hf/^{177}Hf$ and $^{180}Hf/^{177}Hf$ ratios for the reference materials yielded values of 1.46726 ± 0.000008 and 1.88690 ± 0.00007, respectively, and are within 200 ppm of known values based upon atomic masses and abundances (Spencer et al., 2020). Reproducibility of the $^{78}Hf/^{177}Hf$ and $^{180}Hf/^{177}Hf$ ratios are, respectively, 113 and 85 ppm.

5. References

Ehiro, M., Tsujimori, T., Tsukada, K., & Nuramkhaan, M. (2016). Palaeozoic basement and associated cover. In T. Moreno, S. R. Wallis, T. Kojima, & W. Gibbons (Eds.), The geology of Japan (pp. 25–60). London, England: The Geological Society of London.

Ehiro, M., and Takaizumi, Y., 1992, Late Devonian and Early Carboniferous ammonoids from the Tobigamori Formation in the Kitakami Massif, Northeast Japan and their stratigraphic significance, Jour. Geol. Soc. Japan vol. 98, p. 197-204

Fisher, C.M., Vervoort, J.D., Hanchar, J.M., 2014. Guidelines for reporting zircon Hf isotopic data by LA-MC-ICPMS and potential pitfalls in the interpretation of these data. Chemical Geology 363, 125–133. https://doi.org/10.1016/j.chemgeo.2013.10.019

Jackson, S.E., Pearson, N.J., Griffin, W.L., Belousova, E.A., 2004. The application of laser ablation-inductively coupled plasma-mass spectrometry to in situ U–Pb zircon geochronology. Chemical Geology 211, 47–69. https://doi.org/10.1016/j.chemgeo.2004.06.017

Minato, M., Kato, M., Haga, S., 1979, Stratigraphy, Silurian. In Minato, M., Hunahashi, M., Watanabe, J. and Kato, M ends., The Abean Orogeny, Tokai Univ. Press, 56-59

Misaki, A., and Ehiro, M., 2004, Stratigraphy and geologic age of the Middle Permian in the Kamiyasse-Imo district, Southern Kitakami Massif, Northeast Japan, Jour. Geol. Japan, Vol.110, p. 129-145

Okami, K., Ehiro, M., Oishi, M., 1986, Geology of the Lower-Middle Paleozoic around the northern marginal part of the Southern Kitakami Massif, with reference to the geologic development of “Hayachine Tectonic Belt”, 北村信教授記念地質論文集, p.313-330

Okawa, H., Shimojo, M., Orihashi, Y., Yamamoto, K., Hirata, T., Sano, S.I., Ishizaki, Y., Kouchi, Y., Yanai, S. and Otoh, S., 2013. Detrital zircon geochronology of the Silurian–Lower Cretaceous continuous succession of the South Kitakami belt, northeast Japan. Memoir of the Fukui Prefectural Dinosaur Museum, 12, pp.35-78.

Osozawa, S., Usuki, T., Usuki, M., Wakabayashi, J. and Jahn, B.M., 2019. Trace elemental and Sr-Nd-Hf isotopic compositions, and U-Pb ages for the Kitakami adakitic plutons: Insights into interactions with the early Cretaceous TRT triple junction offshore Japan. Journal of Asian Earth Sciences, 184, p.103968.

Paton, C., Hellstrom, J., Paul, B., Woodhead, J., Hergt, J., 2011. Iolite: Freeware for the visualisation and processing of mass spectrometric data. J. Anal. At. Spectrom. 26, 2508–2518. https://doi.org/10.1039/C1JA10172B

Riihimäki, J. and Vehtari, A., 2014. Laplace approximation for logistic Gaussian process density estimation and regression. Bayesian analysis, 9(2), pp.425-448.

Spencer, C.J., Kirkland, C.L., Roberts, N.M.W., Evans, N.J., Liebmann, J., 2020. Strategies towards robust interpretations of in situ zircon Lu–Hf isotope analyses. Geoscience Frontiers 11, 843–853. https://doi.org/10.1016/j.gsf.2019.09.004

Umeda, M., 1996, Radiolarian fossils from the Devonian Onoand Nakazato Formations in the southern Kitakami Belt, Northeast Japan, Earth Science (Chikyu Kagaku), 50, p.311-336

Wiedenbeck, M., Allé, P., Corfu, F., Griffin, W.L., Meier, M., Oberli, F., Quadt, A.V., Roddick, J.C., Spiegel, W., 1995. Three Natural Zircon Standards for U-Th-Pb, Lu-Hf, Trace Element and Ree Analyses. Geostandards Newsletter 19, 1–23. https://doi.org/10.1111/j.1751-908X.1995.tb00147.x

Yoshida, M., Hoyanagi, K., Kondo, H., Inoue, H., Oishi, M., Yoshida, H. and Yanagisawa, Y., 2007. Sequence stratigraphy and organic matter preservation of the Miocene to Pliocene Tatsunokuchi Formation, Iwate, Northeast Japan. Journal of the Sedimentological Society of Japan, 64, pp.21-26.